Graduate School ETD Form 9
(Revised 12/07)

PURDUE UNIVERSITY
GRADUATE SCHOOL
Thesis/Dissertation Acceptance

This is to certify that the thesis/dissertation prepared

By Harpreetsingh Banvait

Entitled OPTIMAL ENERGY MANAGEMENT SYSTEM OF PLUG-IN HYBRID ELECTRIC VEHICLE

For the degree of Master of Science in Electrical and Computer Engineering

Is approved by the final examining committee:

Sohel Anwar (Co-Chair)
Chair

Yaobin Chen (Co-Chair)

Russell Eberhart

To the best of my knowledge and as understood by the student in the *Research Integrity and Copyright Disclaimer (Graduate School Form 20)*, this thesis/dissertation adheres to the provisions of Purdue University's "Policy on Integrity in Research" and the use of copyrighted material.

Approved by Major Professor(s): Sohel Anwar

Yaobin Chen

Approved by: Yaobin Chen 12/3/2009
Head of the Graduate Program Date

Graduate School Form 20
(Revised 6/09)

PURDUE UNIVERSITY
GRADUATE SCHOOL

Research Integrity and Copyright Disclaimer

Title of Thesis/Dissertation:
OPTIMAL ENERGY MANAGEMENT SYSTEM OF PLUG-IN HYBRID ELECTRIC VEHICLE

For the degree of Master of Science in Electrical and Computer Engineering

I certify that in the preparation of this thesis, I have observed the provisions of *Purdue University Executive Memorandum No. C-22,* September 6, 1991, *Policy on Integrity in Research.**

Further, I certify that this work is free of plagiarism and all materials appearing in this thesis/dissertation have been properly quoted and attributed.

I certify that all copyrighted material incorporated into this thesis/dissertation is in compliance with the United States' copyright law and that I have received written permission from the copyright owners for my use of their work, which is beyond the scope of the law. I agree to indemnify and save harmless Purdue University from any and all claims that may be asserted or that may arise from any copyright violation.

Harpreetsingh Banvait
Printed Name and Signature of Candidate

11/24/2009
Date (month/day/year)

*Located at http://www.purdue.edu/policies/pages/teach_res_outreach/c_22.html

OPTIMAL ENERGY MANAGEMENT SYSTEM OF PLUG-IN HYBRID ELECTRIC VEHICLE

A Thesis
Submitted to the Faculty
of
Purdue University
by
Harpreetsingh Banvait

In Partial Fulfillment of the
Requirements for the Degree
of
Master of Science in Electrical and Computer Engineering

December 2009
Purdue University
Indianapolis, Indiana

ACKNOWLEDGMENTS

I would like to gratefully acknowledge my thesis advisors, Dr. Sohel Anwar and Dr. Yaobin Chen for all their guidance and supervision during the entire course of the research and thesis work. I generously express my gratitude to both professors for sharing with me their research experiences. Furthermore, I would like to specially acknowledge Dr. Russell Eberhart for carefully reviewing my thesis and giving me vital information which greatly enhanced the thesis documentation. I also acknowledge the crucial guidance provided by Dr. Xiaohui Hu for applying Particle Swarm Optimization technique to this thesis application.

I would like to extend my special thanks to my research partner Mr. Xiao Lin for his valuable contributions and insightful discussions that led to successful completion of this research.

I would also like to thank my PHEV research team members and co-lab workers at the Mechatronic Research Laboratory, Mr. Emrah Tolga and Mr. Tugsal Umut for their help during the research and support while preparing documentation. I would also like to thank Ms. Valerie Lim Diemer and Ms. Sherrie Tucker for assisting me in formatting this thesis. Finally, I would like to express my gratitude to my parents and my brother for their guidance, support and encouragement during my all life, and my friends.

TABLE OF CONTENTS

Page

Page

LIST OF TABLES

LIST OF FIGURES

Figure Page

Figure Page

ABSTRACT

Banvait, Harpreetsingh. M.S.E.C.E., Purdue University, December 2009. Optimal Energy Management System of Plug-in Hybrid Electric Vehicle. Major Professors: Sohel Anwar and Yaobin Chen.

Plug-in Hybrid Electric Vehicles (PHEV) are new generation Hybrid Electric Vehicles (HEV) with larger battery capacity compared to Hybrid Electric Vehicles. They can store electrical energy from a domestic power supply and can drive the vehicle alone in Electric Vehicle (EV) mode. According to the U.S. Department of Transportation 80 % of the American driving public on average drives under 50 miles per day. A PHEV vehicle that can drive up to 50 miles by making maximum use of cheaper electrical energy from a domestic supply can significantly reduce the conventional fuel consumption. This may also help in improving the environment as PHEVs emit less harmful gases. However, the Energy Management System (EMS) of PHEVs would have to be very different from existing EMSs of HEVs.

In this thesis, three different Energy Management Systems have been designed specifically for PHEVs using simulated study. For most of the EMS development mathematical vehicle models for powersplit drivetrain configuration are built and later on the results are tested on advanced vehicle modeling tools like ADVISOR or PSAT. The main objective of the study is to design EMSs to reduce fuel consumption by the vehicle. These EMSs are compared with existing EMSs which show overall improvement.

In this thesis the final EMS is designed in three intermediate steps. First, a simple rule based EMS was designed to improve the fuel economy for parametric study. Second, an optimized EMS was designed with the main objective to improve fuel economy of the vehicle. Here Particle Swarm Optimization (PSO) technique is used to obtain the optimum parameter values. This EMS has provided optimum parameters which result in optimum blended mode operation of the vehicle. Finally, to obtain optimum charge depletion and charge sustaining mode operation of the vehicle an advanced PSO EMS is designed which provides optimal results for the vehicle to operate in charge depletion and charge sustaining modes.

Furthermore, to implement the developed advanced PSO EMS in real-time a possible real time implementation technique is designed using neural networks. This neural network implementation provides sub-optimal results as compared to advanced PSO EMS results but it can be implemented in real time in a vehicle.

These EMSs can be used to obtain optimal results for the vehicle driving conditions such that fuel economy is improved. Moreover, the optimal designed EMS can also be implemented in real-time using the neural network procedure described.

1. INTRODUCTION

In the recent years, crude oil prices have increased steadily. Additionally, the harmful emissions from automobiles have increased significantly. A large percentage of this crude oil has been used in automobiles as gasoline or diesel. So by reducing the consumption of these crude oil products, it is possible to conserve crude oil and solve both the above stated problems. By replacing the conventional vehicles with electric vehicles (EVs), the crude oil consumption can be reduced to a very large extent. But due to lack of development in infrastructure and lack of technical advancement, EVs cannot currently replace the conventional vehicles.

This transition of vehicles from conventional to electric is expected to be implemented in several steps. Firstly, conventional vehicles will be replaced by hybrid electric vehicles (HEV) which already exist. HEVs are driven by two sources of energy: engine and battery. In the next step, these vehicles are expected to be replaced by plug-in hybrid electric vehicles (PHEV) which can be driven as EVs for a certain range of distance and later on can be driven as HEVs. Finally, these PHEVs would be replaced by EVs as the infrastructure and technical advancement occur. So these inter-transitional steps will help in step by step replacement of current vehicles with EVs which would help in preserving crude oil and also prevent the further degradation of the environment by reducing the harmful emissions from IC engines.

As mentioned before, HEVs have two sources of energy: an electric motor via battery and an IC engine. So by having two degrees of freedom in the energy, flow control has been a larger area of interest for researchers in the past two decades. In HEVs, the battery is charged through the engine, and by regenerative braking while decelerating the vehicle. But as the engine is used to charge the battery and then the battery is used to drive the vehicle, there are large losses in this loop while using fuel. The electric drive mode is very limited for an HEV due to limited battery power. So having a more powerful battery will increase the electric drive range of the vehicle, thus improving fuel economy. Since such a large battery cannot be charged solely by regenerative braking and charging via the engine would not be efficient, it needs to be charged externally by a domestic electric outlet. These HEVs, having an external charging facility for the large battery pack and having a significantly larger EV range, are called plug-in hybrid electric vehicles (PHEVs).

In the past, a lot of research has been done on PHEVs and HEVs. As they have two energy sources many researchers have presented different energy management strategies and also optimized them using various optimization techniques. Dominik Karbowski et al. [1] investigated a control strategy for pre-transmission parallel PHEVs using a global optimization technique based on the Bellman principle. Its main objective was to reduce the losses in engine, motor, and battery. Then they compared their results with the default control strategy given in PSAT [16] for different distances travelled by the PHEV. Aymeric Rousseau et al. [2] used the DIRECT algorithm to obtain some optimized parameters for a rule-based control strategy of pre-transmission parallel PHEVs. They also analyzed the impact of distance travelled by PHEVs with these parameters. Both papers showed that drive cycle and distance travelled impacted their results significantly.

In [3] Qiandong Cao et al. validated the PSAT model for the Toyota Prius PHEV, implemented control strategies to reduce the ON/OFF frequency of the engine by tuning some parameters, and also made the engine to operate in more efficient region in charge depletion (CD) state. Xiaolan Wu et al. [4] used Particle Swarm Optimization (PSO) to

optimize certain parameters of parallel PHEVs for different distances. Fuel economy was the target objective for the problem along with performance and other constraints but he solved the problem as unconstrained PSO. Qiuming Gong [5] used dynamic programming along with intelligent transport system GPS, Geographical Information System (GIS) and advanced traffic flow modeling technique to obtain an optimized power management strategy for a parallel PHEV. Baumann et al. [6] developed load leveling vehicle operation strategy for HEVs and accomplished it using a fuzzy logic controller. He also presented a system integration and component sizing technique. Finally, he simulated implementation in an actual vehicle, both system design and control strategy.

In [7] Yimin Gao et al. presented various rule-based strategies for PHEV passenger cars and analyzed them for fuel consumption. Similarly, Liqing Sun et al. [8] proposed a rule-based control strategy for a parallel PHEV bus model which showed better performance and higher engine efficiency. In [9] Scott Moura et al. used a stochastic Dynamic Programming (DP) technique to obtain optimal power management of a power split PHEV. He implemented it for both blended fuel use strategy and charge depletion/charge sustaining modes and studied the impact of battery size on these control strategies. His results showed that the blending strategy is significantly better for smaller batteries but its effect diminishes for large batteries.

In [10] Borhan et al. showed that predictive control can be implemented for the Energy Management of Power-split HEV which is adaptive to changes, independent of drive cycle and can be implemented in real time. Bin et al. [11] used dynamic programming (DP) to get optimum energy distribution for certain drive cycle. Here DP was implemented in spatial domain while the drive cycle was approximated which showed that time for DP calculations can be reduced to get suboptimal results. Gong et al. [12] used a neural network to detect a highway's on/off ramps patterns by training from data sets and using optimum results for it.

In [13] Mohebbi et al. showed that a neural network based adaptive control method can be used for controlling parallel hybrid electric vehicles. This leads to an online controller that can maximize the output torque of the engine while minimizing fuel consumption. Baumann et al. [14] used artificial neural networks and fuzzy logic to implement a load leveling strategy for intelligent control of a parallel HEV powertrain. Moreno et al. [15] has developed and tested a highly efficient energy management system for HEVs with ultracapacitors using neural networks. They first obtained an optimal control model for it, and then obtained its numerical solution. They tested this new strategy using a neural network which was based on simulation results for different driving cycles.

The following sections include modeling of different hybrid powertrains, special Energy Management Systems (EMSs), simulation results and analysis of those EMSs. Chapter 2 includes modeling of a parallel hybrid powertrain and a power split powertrain which will be used subsequently in simulation of vehicles for the special EMS. Chapter 3 provides details on three different EMSs designed specifically for PHEV and their simulation results for different hybrid powertrains. Chapter 4 contains the simulation results for different EMSs for different drivetrain configurations. Chapter 5 describes a possible real-time EMS so that some EMS mentioned in Chapter 4 can be implemented on the vehicle. Finally, Chapter 5 concludes the thesis by analyzing the results of different EMSs.

2. MODELING

In plug-in hybrid electric vehicles three main types of drivetrain configurations are available:

- Parallel drivetrain: In parallel drivetrain configurations the power can be supplied through the battery and engine separately. Here the torque from both the sources, i.e. battery and engine, are coupled through a torque coupler, speed coupler or torque and speed coupling. Moreover, in a parallel drivetrain the vehicle engine and motor are coupled to the powertrain and can drive the vehicle.

- Series drivetrain: In a series drivetrain configuration the power can be supplied through the battery and engine. When the engine provides the power it is first converted to electrical energy through a generator, then it is converted to mechanical energy through the motor. Furthermore, in a series drivetrain, only the motor is connected to the drivetrain.

- Series/Parallel (Powersplit) drivetrain: In a powersplit drivetrain configuration, both the motor and engine are connected to the powertrain of the vehicle so both can drive it. Additionally, this configuration has another motor/generator. This motor/generator is connected to the engine via a speed coupler. This speed coupler is connected to the motor via a torque coupler which connects to the powertrain as shown in Figure 2.1. Since this powertrain serves as both a series and a parallel powertrain, it is also called the series/parallel drivetrain configuration.

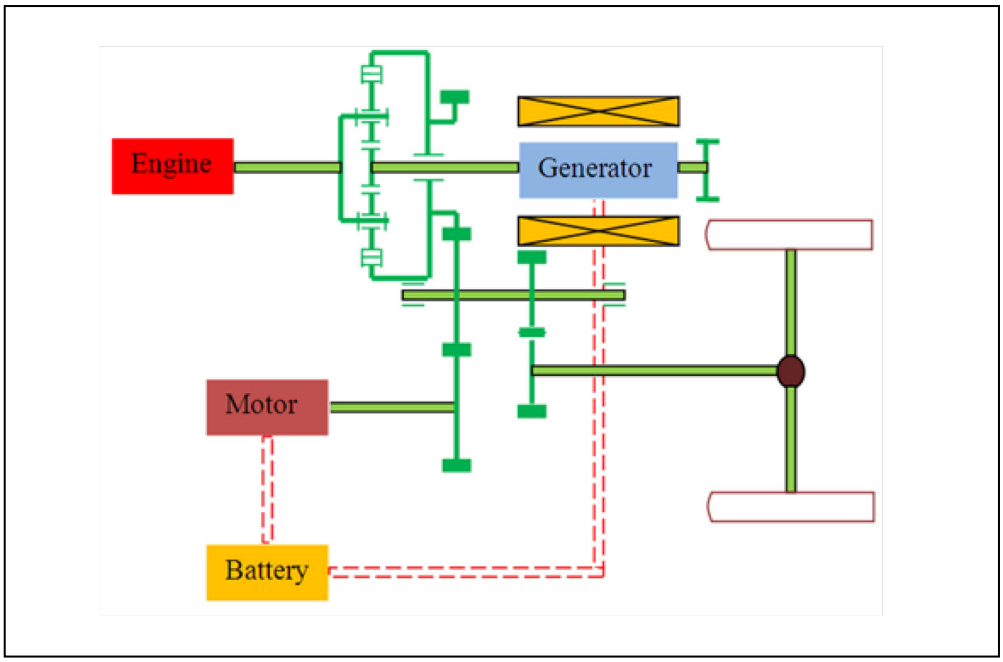

Figure 2.1 Series/Parallel Drivetrain Configuration

In this thesis two different drivetrains, parallel and powersplit, are modeled and simulated for different control strategies. The parallel and powersplit drivetrain configuration models have been used from ADVISOR [17], a modeling and simulation software tool of the National Renewable Energy Laboratory (NREL), for the rule based control strategy. But for the remaining strategies, a more advanced powersplit model from the Powertrain System Analysis Toolkit (PSAT) of Argonne National Laboratory is used. Both models are similar except for certain components. Each component is selected from ADVISOR and PSAT which have preset lookup tables and constants, which are experimentally determined in modeling tools. So in the following subsections details regarding each component of these models are provided.

2.1 Vehicle

The vehicle is modeled by considering the losses in rolling resistance and aerodynamic drag. Furthermore, the force required to overcome ascent is also included

in the model for calculations. When the vehicle moves on roads of different gradients it has large impact on the force required from the vehicle to drive it and can significantly change the accuracy of model. The force required to overcome grade F_g is calculated using Newton's second law using Equation 2.1.

$$F_g = g \times m_v \times \sin(\tan^{-1}(\aleph)) \quad (2.1)$$

where g is gravitational acceleration, m_v is the mass of vehicle in kg and $\aleph$ is road grade in degrees.

As the vehicle moves it is resisted by aerodynamic drag. To calculate this aerodynamic drag it is assumed that lateral wind forces are zero. So the aerodynamic losses F_a are estimated using Equation 2.2.

$$F_a = \sigma \times \mathcal{A} \times C_{air} \quad (2.2)$$

where σ is the air density in Kg/m^3, $\mathcal{A}$ is the frontal area of vehicle in m^2 and C_{air} is the coefficient of aerodynamic drag. All these constants can be determined from experimental results.

Rolling resistance is produced by deformation of the tires at the points of contact with the road. The rolling resistance losses for the vehicle are estimated in this vehicle model using the Equation 2.3.

$$F_{RR} = g \times m_v \times (K_1 + K_2 \times \upsilon) \times \cos(\tan^{-1}(\aleph)) \quad (2.3)$$

where K_1 and K_2 are the coefficients of rolling resistance defined experimentally. Moreover, υ is the velocity of vehicle at previous instant of time in m/s^2.

Using these three loss equations the total force required to drive the vehicle can be approximated using the following Equation 2.4 in the ADVISOR model.

$$F_{REQ} = F_{RR} + F_g + F_a + F_{dmd} \quad (2.4)$$

where F_{dmd} is force demanded for particular vehicle speed.

In the PSAT model the aerodynamic drag and rolling resistance losses are approximated as a second degree polynomial as shown in Equation 2.5.

$$F_{ARR} = \min\left(A_0, \frac{A_0}{0.05}\right)v + A_1 v + A_2 v^2 \quad (2.5)$$

where the constants A_0, A_1 and A_2 are based on experimental results from PSAT. The coefficient of the first term in the above equation is such that it is reduced rapidly at low speeds. It represents the rolling resistance losses. The second term represents higher order co-efficients of rolling resistance and some bearing loss in the axle whereas the third term in this equation represents aerodynamic drag.

Furthermore, the loss due to overcoming grade is calculated using Equation 2.1. So finally the force required is approximated using Equation 2.6.

$$F_{REQ} = F_{ARR} + F_g + F_{dmd} \quad (2.6)$$

2.2 Driver

This component is only used in the PSAT model. It simulates the driver's actions while following the drive cycle and overcoming the losses due to aerodynamic drag, grade and rolling resistance. Here it is assumed that the driver is driving an automatic transmission vehicle. The driver is modeled as a PI controller shown in Equation 2.7. The values of proportional gain K_p and integral gain K_i for a particular driver are determined experimentally in the PSAT tool. The output is torque demand τ_{dmd} and speed demand v which are defined as equations below.

$$\tau_{dmd} = K_p \times e + K_i \int e\, dt \quad (2.7)$$

$$v = v_{DC} \quad (2.8)$$

where

$$Err = v - v_{dmd} \quad (2.9)$$

Moreover, time delay to the torque command generated by the driver is also added to the driver response.

2.3 Wheels and Axle

An axle and pair of wheels connected to the vehicle are modeled together as a single component. In this model the braking torque and inertia corresponding to both the wheels are added for simplification. The wheel and axles are modeled by a kinematic equation as shown in Equation 2.10.

$$\tau_a = \left(F_B - F_{REQ}\right) \times r_w + L_a + I_w \times \frac{d\omega_w}{dt} \tag{2.10}$$

where F_B is the equivalent brake torque of both wheels, r_w is the radius of wheel, I_w is the inertia of wheel, τ_a is the torque acting at axle and ω_w is the wheel rotational velocity.

In ADVISOR the axle losses L_a were obtained from a lookup table which is a function of the tested vehicle mass m_v whereas in the PSAT model these losses are involved in a second order approximated Equation 2.5 in the Vehicle model.

Moreover, PSAT neglects the losses due to slip and assumes that the angular wheel speed is calculated from vehicle speed which is equal to wheel angular speed. But for the ADVISOR model the wheel angular speed is established by Equation 2.11.

$$\omega_w = (\pm s + 1) \times \frac{v_{dmd}}{r_w} \tag{2.11}$$

where s is the resultant slip which is always between -1 and 1. It is estimated using a lookup table which is a function of absolute value of force F_{REQ} and front axle weight, based on experimental data.

2.4 Final Drive

The final drive or differential connects between the wheel axle and the transmission. It distributes the transmission power between the two wheels connected at axle ends. It is modeled similarly in both the PSAT and ADVISOR models. Both of them include the losses due to inertia and final drive. The differential torque τ_d and

differential angular speed ω_d are defined using the dynamics shown in Equations 2.12 and 2.13.

$$\tau_d = \frac{\tau_a}{\Re_d} + I_d \times \frac{d\omega_d}{dt} + L_d \tag{2.12}$$

$$\omega_d = \Re_d \times \omega_w \tag{2.13}$$

In Equations 2.12 and 2.13, L_d is the final drive loss which is approximated using lookup tables. These lookup tables are based on experimental results. Moreover, I_d is the inertia of the differential, ω_d is the angular velocity of the differential and $\Re_d$ is the gear ratio of differential.

2.5 Gearbox

This component is used only in modeling the parallel drivetrain configuration for ADVISOR. This gearbox changes the torque and speeds of the engine to the drivetrain by changing the gear ratio depending on the control system. It considers both the losses due to gearbox inertia and other gearbox losses. The output torque and speed are governed by Equations 2.14 and 2.15.

$$\tau_{gb} = \frac{\tau_d}{\Re_{gb}} + I_{gb} \times \frac{d\omega_{gb}}{dt} + L_{gb} \tag{2.14}$$

$$\omega_{gb} = \Re_{gb} \times \omega_d \tag{2.15}$$

where the gearbox loss is defined by Equation 2.16, I_{gb} is the Inertia of the gearbox and $\Re_{gb}$is the gear ratio of the gearbox which is determined by its control system.

$$L_{gb} = \frac{\varepsilon_1 + \varepsilon_2 + \varepsilon_3 + C_{gb}}{\omega_d \times \Re_{gb}} \tag{2.16}$$

In Equation 2.16 C_{gb} is the constant gearbox losses, ε_1, ε_2 and ε_3 variables are as shown in Equations 2.17-2.19.

$$\varepsilon_1 = |\tau_d| \times \left(C_{o\_t} + \frac{C_{i\_t}}{\Re_{gb}} \right) \tag{2.17}$$

$$\varepsilon_2 = |\tau_d| \times C_{o\_p} \times \omega_d \quad (2.18)$$

$$\varepsilon_3 = \omega_d \times \left(C_{o\_s} + \Re_{gb} \times C_{i\_s}\right) \quad (2.19)$$

In the above Equations 2.17 – 2.19, C_{i_t}, C_{i_s}, C_{o_t} and C_{o_p} are input torque coefficient, input speed coefficient, output torque coefficient and output power coefficient respectively.

2.6 Continuous Variable Transmission

This component is present only in the powersplit drivetrain configuration in both the ADVISOR and PSAT models. As mentioned before, for speed coupling a planetary gear set is used. This planetary gear is torque coupled with the motor to provide the output to the drivetrain. In the planetary gear set the sun gear was connected to Motor 2 which can be called a generator since it mainly converts mechanical energy from the engine into electrical energy. Furthermore, the carrier gear of the planetary gear set is connected to engine. Finally, the ring gear of this planetary gear set is connected to Motor 1 which also drives the vehicle.

In the ADVISOR model the engine speed ω_e and engine torques τ_e are controlled by the vehicle control system. Furthermore, the ring torque τ_r and ring speed ω_r are defined equivalent to differential torque and differential speed. Equations 2.20 – 2.23 are used to model the continuously variable transmission and are based on kinematic equations of planetary gear set. These equations define motor torque τ_m, motor speed ω_m, generator torque τ_g and generator speed ω_g.

$$\tau_m = \tau_r - \beta_1 \times \tau_e \quad (2.20)$$

$$\omega_m = \omega_r \quad (2.21)$$

$$\tau_g = \beta_2 \times \tau_e \quad (2.22)$$

$$\omega_g = \beta_3 \times \omega_e - \beta_4 \times \omega_m \quad (2.23)$$

where,

$$\beta_1 = \frac{\Re_r}{\Re_r + \Re_S} \tag{2.24}$$

$$\beta_2 = -\frac{\Re_S}{\Re_r + \Re_S} \tag{2.25}$$

$$\beta_3 = 1 + \frac{\Re_r}{\Re_S} \tag{2.26}$$

$$\beta_4 = \frac{\Re_r}{\Re_S} \tag{2.27}$$

In Equations 2.24 – 2.27 $\Re_S$ and $\Re_r$ are sun gear ratios and ring gear ratios.

In the PSAT model the motor torque is given by Equation 2.28 below instead of Equation 2.20. For further information on this equation and constants α_1, α_2 and α_3 refer to [16].

$$\tau_m = \tau_r - \frac{(\alpha_1 \tau_g + \alpha_2 \tau_e)}{\alpha_3} \tag{2.28}$$

2.7 Motor

The motor model used in both the ADVISOR and PSAT models for parallel and powersplit drivetrain configurations is the same. The model of the motor includes the effects of losses in motor inertia and motor's torque speed-dependent capability. The power losses in motor are specified for the motor using lookup tables from experimental results in PSAT. The motor is modeled using the dynamic equation below.

$$\tau_{total\_m} = \tau_m + I_m \times \frac{d\omega_m}{dt} \tag{2.29}$$

$$\omega_m = \omega_{REQ} \tag{2.30}$$

Moreover, the motor's maximum torque is also enforced using a lookup table which is indexed by motor speed. The motor is commanded such that motor current does not exceed the maximum current limit. The ADVISOR model of motor has a more detailed thermal model. For more information refer to ADVISOR documentation [17]. In PSAT

only heat index was calculated which was used to define the maximum motor torque constraint.

2.8 Engine

In both of the simulation tools ADVISOR and PSAT it is assumed that gasoline is used as fuel to produce mechanical energy. The required torque and speeds are obtained from the drive cycle. The engine speed and torques are calculated in the vehicle control system module and sent as commands to the engine controller module. It controls the engine to operate it in desired torque and speed ranges. Here the engine is not modeled as a very complex dynamical system but for control analysis at vehicle level it considers only the inertial losses and thermal losses. Moreover the mechanical or electrical accessories loads L are assumed to be a constant. The torque and speeds available from the engine are defined as the following equations where I_e is engine inertia.

$$\tau_{total\_e} = \tau_e + I_e + L \tag{2.31}$$

$$\omega_{REQ\_TOTAL} = \omega_{REQ} \tag{2.32}$$

Based on engine operating torque and speed the fuel consumption is obtained from the 2-D lookup table as a function of engine torque and speed. Similarly exhaust flow rate, hydrocarbons (HC), carbon monoxide (CO), oxides of nitrogen (NO_X), particulate matter (PM), and oxygen content in exhaust gases from the engine are estimated using the 2-D lookup table maps which are functions of both engine torque and speed. All these lookup tables were obtained using experimental results for specific engines which were already defined in both the PSAT and ADVISOR models. Furthermore, the engine model in the ADVISOR model has a thermal model to monitor the heat transfer process. For more details on calculations for the thermal model of engine refer to ADVISOR documentation [17].

2.9 Battery

The battery is modeled in the both PSAT and ADVISOR models as an open circuit voltage model. The battery pack is composed of cells arranged in specific patterns of series and parallel connections. The power losses in the battery are calculated using I^2R losses by Columbic inefficiency. The battery state of charge (SOC) is computed from the power demand at the bus using Equation 2.33.

$$SOC = \frac{(\gamma_{max} - \gamma)}{\gamma_{max}} \tag{2.33}$$

where,

$$\gamma = \int_{t=k=1}^{t=k} I\, dt + \gamma_{max} \times (1 - SOC_{k=1}) \tag{2.34}$$

As mentioned above the battery is modeled as an equivalent circuit consisting of an open circuit voltage which is in series with the battery internal resistance R_b.

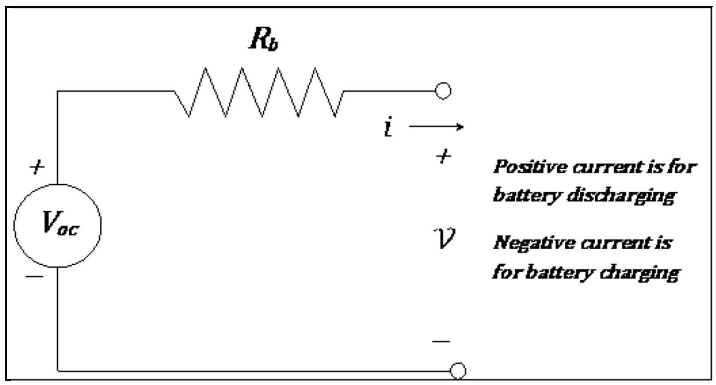

Figure 2.2 Equivalent Circuit Diagram for Energy Storage System

Here the bus current is obtained by solving the quadratic Equation 2.36 for the current and using Kirchhoff's voltage law in battery equivalent open circuit diagram.

$$V = \frac{P_b}{I} = V_{OC} - R_b \times I \tag{2.35}$$

$$\Rightarrow R_b \times I^2 - V_{OC} \times I + P_b = 0 \tag{2.36}$$

Solving this Equation 2.36 we get,

$$I = \frac{V_{OC} - \sqrt{V_{OC}^2 - 4 \times R_b \times P_b}}{2 \times R_b} \tag{2.37}$$

where,

$$V_{OC} = Lookup\ Table\ (SOC, Tmp) \tag{2.38}$$

$$R_b = Lookup\ Table\ Charge\ or\ Discharge\ (SOC, Tmp) \tag{2.39}$$

Similarly the bus voltage is also obtained using Kirchhoff's law as shown in Equation 2.40.

$$V = V_{OC} - R_b \times I \tag{2.40}$$

The maximum power limit required is calculated by Equation 2.41.

$$P_{max} = V_{bus} \times \frac{V_{oc} - V_{bus}}{R_b} \tag{2.41}$$

Using Equations 2.37 and 2.40 the voltage and current of the battery are estimated. Moreover by using Equation 2.41 the maximum power drawn from battery is approximated in the ADVISOR model whereas in the PSAT model this maximum power drawn by battery is evaluated using the lookup tables provided along with the battery specifications.

3. ENERGY MANAGEMENT SYSTEMS

HEVs consist of two different energy sources, a battery and an engine. The power required to drive the vehicle can be obtained from either the battery or the engine. These two energy flow paths can be controlled to run the vehicle efficiently. The Energy Management System (EMS) is responsible for management of the energy flow from these two sources by sending commands to the battery, motor and engine. For HEVs, these sources of energy can be controlled so that energy flow from both sources is efficient. The PHEV battery is charged from an external power supply which is much cheaper than gasoline. The EMS of a PHEV is designed such that the vehicle makes more use of the battery than the engine, to drive the vehicle. Various researchers have worked to design such vehicle level EMSs, and have even optimized them.

In this Section the designs of three different EMSs are described. First, is a rule based EMS for a parallel and powersplit drivetrain. Second, is a Particle Swarm Optimization (PSO) based optimum EMS for a powersplit drivetrain. Finally, an advanced optimized EMS using PSO for a powersplit drivetrain is explained. The following three subsections include details regarding these three EMSs.

3.1 Rule Based EMS

PHEVs have a higher capacity battery that is initially charged by an electric outlet. Since this electrical energy is much cheaper, maximum use of this battery should be made to reduce the fuel consumption by the engine hence resulting in lower driving cost. In this rule based EMS the maximum power is drawn from the battery via motor to drive the vehicle. The rest of the power if demanded is provided by engine.

This rule based strategy was designed and implemented for the simulation of both the parallel drivetrain and the powersplit drivetrain. The parallel drivetrain configuration uses a gearbox so only speed was selected as a command signal to the engine while the operating torque of the engine is dependent on the driving cycle and battery SOC. The powersplit configuration has a continuous variable transmission in the powertrain. So engine speed and torque both are controlled along with motor speed and torques to drive the vehicle while satisfying the desired driving performance. Moreover in both powertrains the engine torque is also dependent on the battery SOC. Here the engine is turned ON and OFF according to a certain set of rules which are mentioned as follow.

1. If SOC of the battery is below the lower limit of SOC and positive power is required by the vehicle then the engine must be turned ON.
2. If the SOC of the battery is above its lower limit and the power requested by the vehicle is less than the maximum power that can be provided by the motor but positive then the engine must be turned OFF.
3. If the SOC of the battery is above its lower limit and the power requested by the vehicle is more than the maximum power that can be provided by the motor but positive then the engine must be turned ON.
4. If the power requested by the vehicle is negative and the state of charge of the battery is below its upper limit then the engine must be turned OFF.

In charge sustaining mode the engine and battery are used such that the SOC of the battery is maintained at the desired value irrespective of the load changes in the vehicle. Whereas in charge depletion mode maximum use of battery, is made while limiting the use of the engine which results in rapid reduction in SOC of the battery. In this rule based strategy vehicle operating modes are based on the charge depletion and charge sustaining operation modes. The following rules define the operating modes of the vehicle.

a) If the SOC of the battery is above its lower limit and the power required by the vehicle can be fulfilled by the motor alone then the vehicle is driven in Electric Vehicle (EV) mode.
b) If the SOC of the battery is above its lower limit and the power required by the vehicle cannot be provided by the motor alone then the engine is used to provide the rest of the power to drive the vehicle.
c) If the SOC of the battery is below its lower limit and the power required by the vehicle is less than the power that can be generated by the engine at its optimal operating point then the engine is operated at its optimal operating point and the rest of the power is used to charge the battery.
d) If the SOC of the battery is below its lower limit and the power required by the vehicle is more than the power that can be generated by the vehicle at the optimal operating point then the engine power is used to drive the vehicle.
e) If the SOC of the battery is lower than the upper limit and the required power is negative then this negative power is used to charge the battery directly through regenerative braking.

For the parallel drivetrain configuration the additional torque required from the engine is calculated using the following equation.

$$\tau_{SOC} = \frac{\left(\gamma - \left(\frac{\gamma_h + \gamma_l}{2}\right)\right)}{\left(\frac{\gamma_h - \gamma_l}{2}\right)} \times \tau_{Max\_SOC} \tag{3.1}$$

In the above Equation 3.1 the τ_{SOC} is the torque required to charge the vehicle, γ is SOC, γ_h is the SOC upper limit, γ_l is the SOC lower limit and τ_{Max_SOC} is the maximum charging torque. For the powersplit configuration the power demanded from the engine is estimated using the following equation.

$$P_{SOC} = {I_{ch}}^2 R_b \pm V_{OC} I_{ch} \tag{3.2}$$

In Equation 3.2 I_{ch} is the current required to charge the battery and other variables are defined in Chapter 2.

Moreover, for the optimum operating points of the engine the optimum speed was obtained from the demanded load power using the predefined lookup table in ADVISOR. The subsequent optimum torque is obtained from the demanded load power and optimum speed.

3.2 Particle Swarm Optimization Based EMS

In Section 3.1 the EMS was rule based so it did not promise to provide optimum results. To obtain optimum results we can use gradient based algorithms. But these algorithms depend on the gradients to find the optimum solution and don't always give the global minimum or maximum as a solution. Moreover it is very hard to find a derivative of complex non-linear problems. So to find the global minimum solution, derivative free algorithms such as Genetic Algorithm (GA), DIRECT, Dynamic Programming, Particle Swarm Optimization (PSO), etc., can be used. They do not depend on gradients to find the solution to problems. One main advantage of such derivative free algorithms is that they have a tendency to provide global minimum solutions and don't get stuck in local minimum solutions as the gradient based algorithms do. To obtain the near optimum results for this EMS, PSO is used.

PSO was developed by Dr. James Kennedy and Dr. Russell Eberhart [18]. It is based on a stochastic optimization technique and the social behaviors of bird flocking or fish schooling. It is very similar to other evolutionary computation techniques like Genetic Algorithms (GAs). But it does not have evolution operators like mutation and crossover. In the PSO, a group of particles are randomly initialized with their own position and velocity in the multidimensional problem space. Each particle in this space is a possible solution to the problem. The PSO was developed by Dr. Eberhart and Dr. Kennedy in two versions, a Global version and a Local version [19]. This article showed

that the global solution has a tendency to converge at the local optimum values for certain problems. It also showed that the global version takes less number of iterations to reach a convergence as compared to the local version. In this application, it is required to obtain an optimum solution at an interval of 1 second hence the global version of the PSO is selected. In the algorithm the fitness or objective function is evaluated for each particle, at each time interval and an update is made to the best global solution. These particles then flow generally towards the better solution using the equations defined by the PSO which are as follows:

$$V(k+1) = w \times V(k) + c_1 \times r_1 \times \big(pBest(k) - x(k)\big) + c_2 \times r_2 \times \big(gBest(k) - x(k)\big) \tag{3.3}$$

$$x(k+1) = x(k) + V(k+1) \tag{3.4}$$

Equation 3.4 is the position of the particle for the next iteration based on its velocity in the current iteration which is obtained using Equation 3.3. In Equation 3.3 $pBest$ is the particle's own best position and $gBest$ is the global best position. $gBest$ is determined by comparing the $pBest$ of all particles. c_1 is the cognition learning rate which controls the velocity increase or decrease depending on the particle's personal best, whereas c_2 is the social learning rate of the particle which controls the velocity increase or decrease depending on the $gBest$. w is the inertial weight which enhances the performance of PSO in various applications[20]. r_1 and r_2 are random numbers between 0 and 1 Each particle is updated and moved in directions at every time step using Equations 3.3)and 3.4. Finally this iterative process ends when optimal solution is obtained and all the particles converge or a maximum number of iterations occur,. A major advantage of PSO is that it requires very few parameters mentioned above to be adjusted to obtain optimum solutions to the problems.

This PSO technique was developed for unconstrained optimization problems. However different versions of the PSO technique have been developed in the past which can be used for constrained optimization problems. In [21] Gregorio Toscano proposed a

PSO approach with variation in velocity computation formula, turbulence operator and different mechanism to handle the constraints. The penalty function approach as shown by Konstantinos Parsopuulos [22] is another approach used for solving constrained optimization problems with PSO. Here an additional penalty function is added to the fitness function and then the problem is solved as an unconstrained problem.

In [20] Hu and Eberhart suggest a method with some modification in the PSO algorithm used for unconstrained optimization problems so that it can be used for constrained optimization problems. They suggest two changes in the PSO algorithm. First, all the particles have to be reinitialized until they are initialized in the feasible space. Second, when updating the $gBest$ and $pBest$ variables for each iteration, only the feasible points are assigned as $gBest$ and $pBest$. So the PSO algorithm always starts with all the particles in the feasible solution space. Even if some particles go into unfeasible solution space while it is running but they always return to the feasible solution space region because the $gBest$ and $pBest$ which influence the motion of particles in the space are always in the feasible solution space.

Here the problem for obtaining the optimum solution for the EMS of PHEV is a constrained optimization problem. In this problem the near-efficient operating points of the engine are determined using PSO as suggested by Hu and Eberhart [20]. To achieve this, twenty particles are defined in a two dimensional space of engine speed and engine torques. All these optimum points always satisfy the performance constraints and other constraints using the modified algorithm suggested by Hu and Eberhart after accounting for the losses in the powertrain. The PSO parameters w, c_1 and c_2 were defined as suggested by Hu in [20] and in Table 3.1. The PSO algorithm flowchart for constrained optimization is as shown in Figure 3.1.

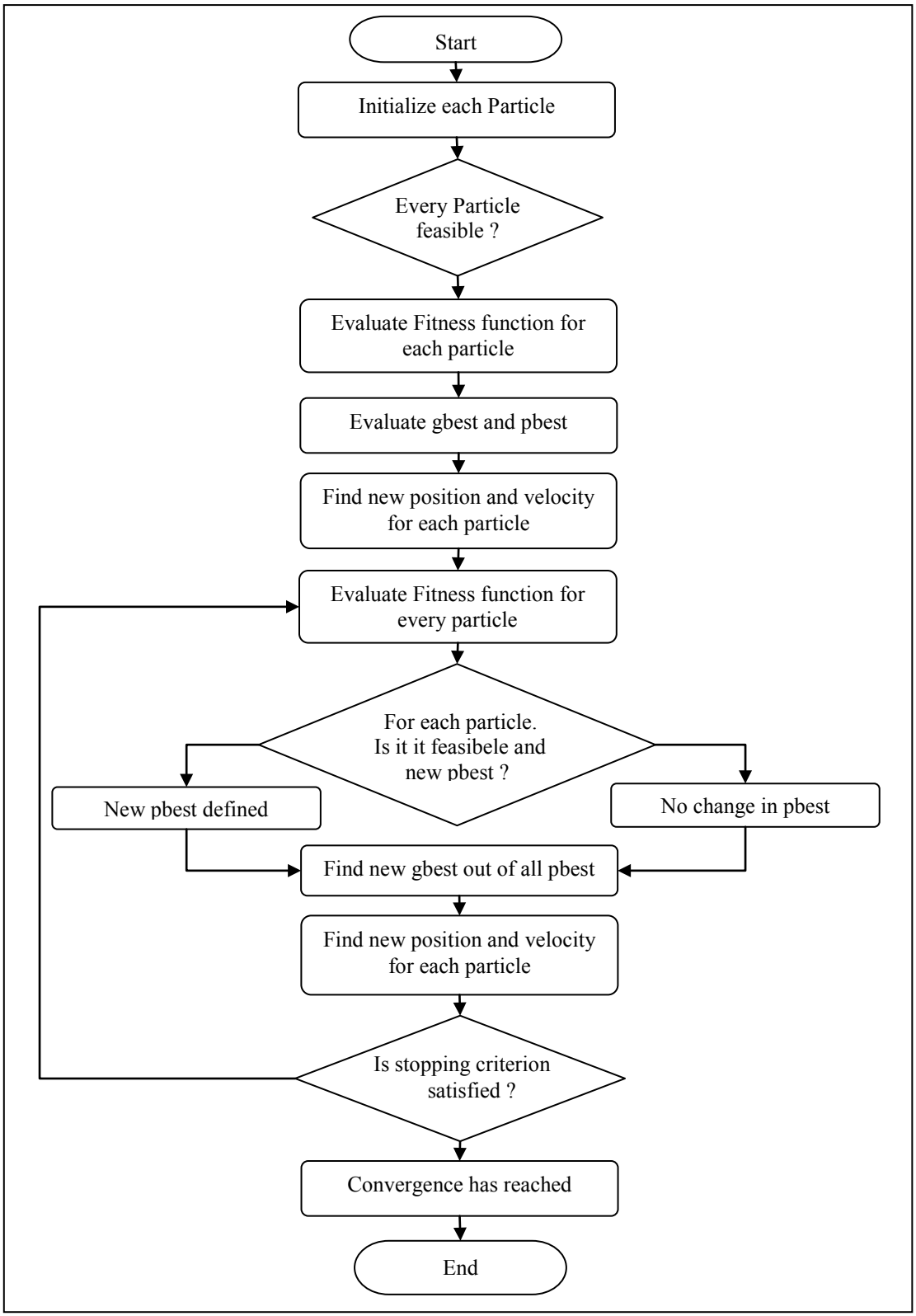

Figure 3.1 Flowchart of Constrained PSO Algorithm

Table 3.1 PSO Parameters

PSO Parameters	Value
w	$0.5 + \frac{random()}{2}$
c_1	1.49445
c_2	1.49445
Dimension	2
Number of Particles	20

3.2.1 Problem Formulation

The powersplit configuration has a planetary gear set which can provide an infinite number of gear ratios. Hence the engine can be operated at any speed and torque while satisfying the required torque and speed by the vehicle to follow the drive cycle. So the engine can be operated in the proximity of its most efficient operating range, and the fuel economy of the vehicle can be improved while satisfying the required performance.

To find this best engine operating point the optimization problem was defined. The main objective of the research project is to increase the fuel economy of the vehicle while satisfying the performance required by the vehicle. The objective function to minimize fuel consumption by the vehicle for the optimal energy management system is defined in Equation 3.5.

$$Min: \ \vartheta\ (\tau_e, \omega_e) \tag{3.5}$$

The equivalent fuel consumption (ϑ) is obtained in Equation 3.6.

$$\vartheta\ (\tau_e, \omega_e) = \int_{t=k-1}^{t=k} \dot{m}_e(\tau_e, \omega_e)\, \mathrm{d}t + \ \sigma(\gamma_k) \tag{3.6}$$

This equivalent fuel consumption is the sum of the fuel consumed by the engine to drive the vehicle and the SOC equivalent fuel (σ). The SOC equivalent fuel is defined to evaluate energy consumption from the battery. It is evaluated using Equation 3.7.

$$\sigma(\gamma_k) = -\psi \times \mathcal{V} \times \mathcal{C}_{max} \times (\gamma_k - \gamma_{k-1}) \tag{3.7}$$

In Equation 3.7 ψ is the average fuel consumption by the engine which is 250 g/Kwh selected from the engine Brake Specific Fuel Consumption (BSFC) map, $\mathcal{V}$ is the voltage of battery, γ_{pre} is the previous SOC and $\mathcal{C}_{max}$ is the maximum capacity of the battery. The SOC equivalent fuel is positive if the battery is supplying power otherwise it is negative. Here the efficiency for electrical to mechanical energy conversion is taken into consideration using the lookup tables.

The energy management system for the powersplit configuration is very complex. The objective function defined is subjected to several constraints. These constraints are as follows:

$$0 < \tau_e < \tau_{e\max}(\omega_e) \tag{3.8}$$

$$\omega_{emin} < \omega_e < \omega_{emax} \tag{3.9}$$

$$-\omega_{gmax} < \omega_g < \omega_{gmax} \tag{3.10}$$

$$-\tau_{gmax}(\omega_g) < \tau_g < \tau_{gmax}(\omega_g) \tag{3.11}$$

$$-\omega_{mmax} < \omega_m < \omega_{mmax} \tag{3.12}$$

$$-\tau_{mmax}(\omega_m) < \tau_m < \tau_{mmax}(\omega_m) \tag{3.13}$$

$$\gamma_{min} < \gamma < 1 \tag{3.14}$$

$$-P_C(\gamma) < P_b < P_D(\gamma) \tag{3.15}$$

Along with these constraints, performance constraints in Equations 2.22 and 2.23 are also included so that vehicle will always achieve the desired performance. All of these constraints must be satisfied to have a feasible solution to the problem. All the variables including generator speed (ω_g), generator torque (τ_g), motor speed (ω_m), motor torque (τ_m), power required from battery (P_b) and SOC (γ) are calculated using the

equations in Chapter 2 for the given engine speed (ω_e) and engine torque (τ_e). The limits on these variables were either obtained using lookup tables or constant which were obtained from the component specifications. In Equation 3.15 P_C is the charge/discharge limit and P_D is the discharge limit of the battery. All these variables are obtained using the simplified model. The simplified model consisted of a driver model, a vehicle model, a final drive model, a CVT model and a battery model. The modeling details of the battery model, the final drive model and the driver model are provided in Chapter 2. The vehicle model consists of Equations 2.5 and 2.6, whereas the CVT model consists of Equations 2.28, 2.21, 2.22 and 2.23.

The hierarchical implementation structure for this EMS is shown in Figure 3.2.

3.3 Advanced Optimized EMS using PSO

This Advanced Optimized EMS is similar to the Particle Swarm Optimization based EMS as described in Section 3.2 for the powersplit drivetrain. This EMS is also based on optimum results obtained from PSO. The PSO used is shown in the flow chart shown in the flowchart of Figure 3.1. The PSO parameters used for optimization are also similar to the Section 3.1 PSO parameters.

The implementation of PSO for the powersplit drivetrain PHEV is shown in the diagram below.

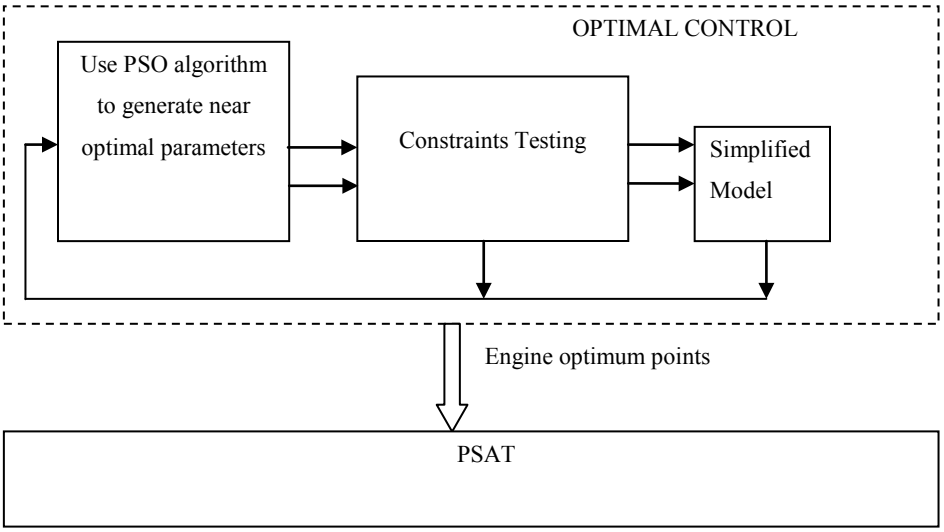

Figure 3.2 Hierarchical Structure of EMS for Powersplit PHEV

As shown in Figure (3.2) the engine optimum points were calculated for the optimal control section using the PSO algorithm and the simplified model. The simplified model was used to estimate the ring gear speed of planetary gear $\omega_r(t)$, ring gear torque $\tau_r(t)$ of the planetary gear, and SOC γ. The simplified model used in this EMS is same as the simplified model used in Section 3.2.1. The entire calculation was repeated for each time step of the drive cycle demands. The optimization process used a simplified model using the equations described in Chapter 2. Finally, the optimum engine operating points were given as input commands to the PSAT model and then analyzed.

The objective function and problem formulation were different from the problem formulation described in Section 3.2.1

3.3.1 Problem Formulation

As mentioned before the powersplit configuration is used which has a continuously variable transmission. For a given drive cycle, vehicle speed $v_{\mathrm{veh}}(t)$ is obtained from the profile, while the total required torque at wheel $\tau_{\mathrm{w}}(t)$ is calculated from the simplified model. Both variables are supposed to be known $\forall t \in [0 \cdots (\mathrm{N}-1)]$.

The objective function for this problem is defined as follows:

$$\int_{t=n}^{t=n+1} \begin{pmatrix} \sigma_e(t)\dot{m}_e\big(\omega_e(t),\tau_e(t)\big) + \\ f\big(soc(t)\big)\dot{m}_b(t) \end{pmatrix} dt + p_1 + p_2 \tag{3.16}$$

where,

$$\dot{m}_b(t) = \frac{\big(\omega_m(t).\tau_m(t) + \omega_g(t).\tau_g(t)\big)}{\vartheta} \aleph \tag{3.17}$$

$$p_1 = \begin{cases} \mu_1 & soc_{n+1} < soc_l \; and \; soc_{n+1} < soc_n \\ 0 & \text{else} \end{cases} \tag{3.18}$$

$$p_2 = \begin{cases} {\mu_2}^{\alpha+1} & \sigma_e(t) \neq \sigma_e(t-1) \\ 0 & \sigma_e(t) = \sigma_e(t-1) \end{cases} \tag{3.19}$$

In Equation 3.16 $\dot{m}_e$ and $\dot{m}_b$ are the fuel consumption rate of the engine and the rate of equivalent fuel consumption of the battery. Therefore, the integral part of Equation 3.16 is the equivalent fuel consumption that takes both gasoline usage of the engine and the electrical usage of the battery into consideration. Furthermore, an SOC weighting factor was introduced to determine the energy distribution policy between the engine and the battery. The weighting factor is shown in Figure 3.3.

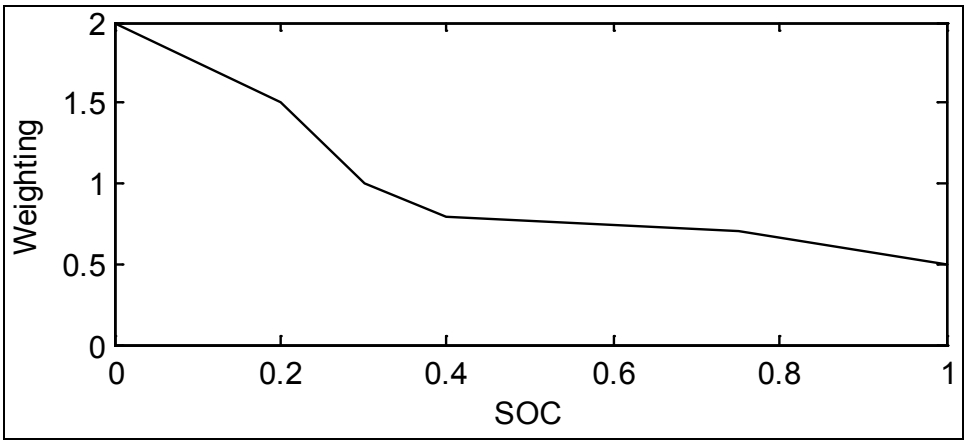

Figure 3.3 Energy Distribution Weighting Factor

Figure 3.3 shows that when SOC is high, the weighting factor was as low as 0.5 which results in depleting more energy from the battery and less energy from the engine.

This weighting factor was then gradually increased to 1 and then to 2. When SOC is low the weighting factor has values higher than 1 so engine usage is increased and battery usage is reduced.

In Equation 3.16 p_1 is the added penalty cost with regard to the battery SOC as described in Equation 3.18. Here soc_l is the allowed SOC value. When the SOC value is was below soc_l a corresponding penalty cost p_1 is added to the objective value to prevent the battery from being over discharged. Hence, the vehicle is in SOC sustain mode which maintains battery SOC around some target value. p_2 is penalty cost added to prevent frequent engine ON/OFF changes. This extra penalty cost significantly reduced engine ON/OFF switches. It is defined by Equation 3.19. If the current engine status is changed then the duration of previous engine status α is used to decide the exact penalty cost according to different situations. But if there is no change in engine status then no penalty cost is added to the objective function.

All the variables in p_1, p_2 and the weighting factor are empirically determined and selected. More details regarding the values of the variables are shown in Table 3.2.

Table 3.2 Objective Function Parameters

Parameters	Values
א	240 g/Kwh
ϑ	2.78×10^{-7}
μ_1	0.25
μ_2	0.5

Moreover, this objective function is also subjected to various constraints which are described below.

$$0 \leq \omega_{\mathrm{e}}(t) \leq \omega_{\mathrm{e,max}} \tag{3.20}$$

$$0 \leq \tau_{\mathrm{e}}(t) \leq \tau_{\mathrm{e,max}}\left(\omega_{\mathrm{e}}(t)\right) \tag{3.21}$$

$$\omega_{\mathrm{m,min}} \leq \omega_{\mathrm{m}}(t) \leq \omega_{\mathrm{m,max}} \tag{3.22}$$

$$\tau_{\mathrm{m,min}}\left(\omega_{\mathrm{m,}}(t), soc(t)\right) \leq \tau_{\mathrm{m}}(t) \leq \tau_{\mathrm{m,max}}\left(\omega_{\mathrm{m}}(t), soc(t)\right) \tag{3.23}$$

$$\omega_{\mathrm{g,min}} \leq \omega_{\mathrm{g}}(t) \leq \omega_{\mathrm{g,max}} \tag{3.24}$$

$$\tau_{\mathrm{g,min}}\left(\omega_{\mathrm{g,}}(t), soc(t)\right) \leq \tau_{\mathrm{g}}(t) \leq \tau_{\mathrm{g,max}}\left(\omega_{\mathrm{g}}(t), soc(t)\right) \tag{3.25}$$

$$soc_{\mathrm{min}} \leq soc(t) \leq soc_{\mathrm{max}} \tag{3.26}$$

In addition to these equations the vehicle performance constraints are also included as given by Equations 2.22 and 2.23. In Equations 3.20-3.26 τ_{e}, τ_{m} and τ_{g} are the engine torque, motor torque and generator torques, while ω_{e}, ω_{m} and ω_{g} are engine speed, motor speed and generator speeds respectively. The τ_{e} and ω_{e} are obtained from the optimum results from PSO whereas the other four variables are determined using the equations from Chapter 2. Furthermore, soc_{min} and soc_{max} are the minimum and maximum SOC values which are obtained from the battery's electrical constraints. The remaining maximum and minimum values of all the torques and speeds are obtained from the specifications of the motor, generator and engine. Some of them are constants whereas others are in lookup tables obtained from their specifications.

4. SIMULATION

4.1 Rule-Based EMS Simulation

The Rule based EMS was implemented in ADVISOR (Advanced VehIcle SimulatOR) software v2.1. ADVISOR is a vehicle modeling tool designed by NREL (National Renewable Energy Laboratory) using the Simulink model, test data, and script m-files of MATLAB. It is used to simulate vehicle performance and fuel economy of conventional, electric, and hybrid vehicles for different drive cycles and driving conditions. Each component model of the vehicle is empirically designed based on input and output relationship of drivetrain components derived from their laboratories. For more information regarding ADVISOR refer to ADVISOR Documentation [17].

In this section the rule based EMS and ADVISOR default strategies were tested on a parallel drivetrain as well as a powersplit drivetrain using the models present in ADVISOR. The relevant components of the model were designed according to the details mentioned in Chapter 2.

4.1.1 Simulation for Parallel Drivetrain

The following sections provide details regarding the model setup and simulation results based on the proposed Rule-Based EMS for parallel drivetrain.

4.1.1.1 Simulation Setup

The rule-based EMS was implemented in a parallel powertrain model after some modifications according to the requirements of the EMS. This HEV was converted into a PHEV by assuming that 100% efficiency is achieved while charging the battery from a domestic power supply. Moreover, the HEV parallel powertrain model in ADVISOR was modified into PHEV by increasing the battery size as shown in Tables 4.1 and 4.2. The engine ON/OFF switching and engine torque control were designed according to strategy demands. Moreover, the power routing in the planetary gear set was also designed according to the requirements. The control parameters for this control strategy were set inside the model according to the table below:

Table 4.1 Model and Parameter Values Used for Parallel Model and Rule Based EMS

Model\Variable	Name\Value
Engine	FC SI 41 emis 41 kW
Motor	AC 75 kW
Battery	LI7 Li- Ion
Battery Max Capacity	6.3 kwh
Initial Conditions	Hot Temp Conditions
Initial SOC	95%
SOC High	90%
SOC Low	35%

The parallel control strategy is described in detail in the Appendix section. For simulating the parallel control strategy on the parallel powertrain model the control parameters were defined as shown in the following table.

Table 4.2 Model and Parameter Values Used for Parallel Drivetrain Vehicle with Parallel Control Strategy

Model\Variable	Name\Value
Engine	FC SI41 emiss 41 kW
Motor	MC AC 75
Battery	LI7 Li-Ion
Initial Conditions	Hot Temp Conditions
Initial SOC	95%
SOC High	90%
SOC Low	35%
Electric Launch Speed Limit	30 MPH
OFF Torque Fraction	20%
Min Torque Fraction	40%
Charge Torque	15.25 Nm

Moreover all remaining parameters for the parallel drivetrain were the default parameters according to the "Parallel_default_in" in the vehicle model in ADVISOR.

The parallel model was simulated for UDDS drive cycle. It was the standard EPA drive cycle designed by EPA which is used for simulating the Urban Driving experience and testing different vehicles. The various characteristics of one UDDS drive cycle are shown in the following table:

Table 4.3 UDDS Drive Cycle Characteristics

Characteristic	Value
Distance	7.45 miles
Time	1369 s
Max speed	56.7 mph
Average speed	19.58 mph
Max Acceleration	4.84 ft/s^2
Max Deceleration	-4.84 ft/s^2
Average Acceleration	1.66 ft/s^2
Average Deceleration	-1.9 ft/s^2
Idle time	259 s
Number of stops	17

4.1.1.2 Simulation Results and Analysis

The same simulation model was used to implement both the rule based EMS and the parallel control strategy. The model was then simulated for five consecutive UDDS or EPA drive cycles since one drive cycle did not provide a good comparison and maximum capability of a PHEV vehicle. The total distance traveled by the vehicle was 37.2 miles. The speed attained by the vehicle while following the desired drive cycle is shown in Figure 4.1 below.

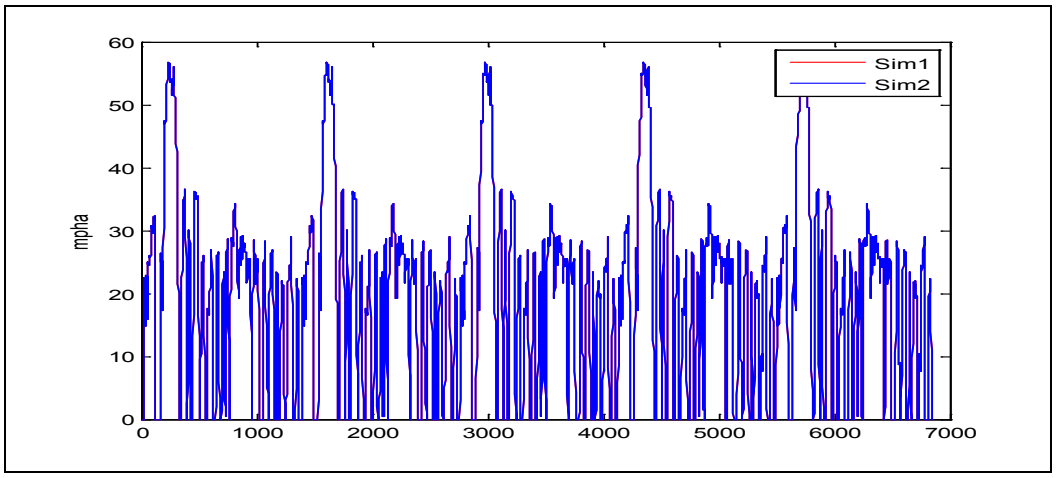

Figure 4.1 EPA Drive Cycles

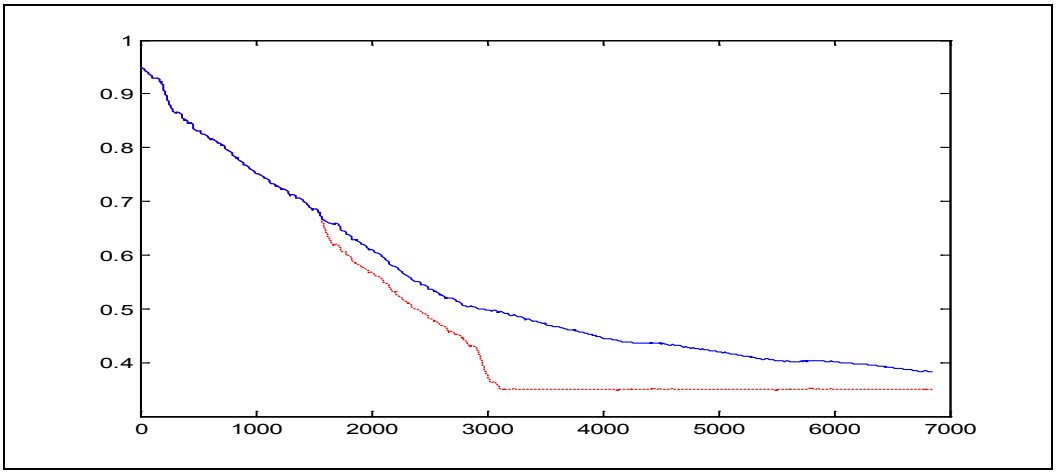

Figure 4.2 SOC of Parallel Control Strategy (blue and continuous) and SOC of Rule Based EMS PHEV Strategy (red and dotted)

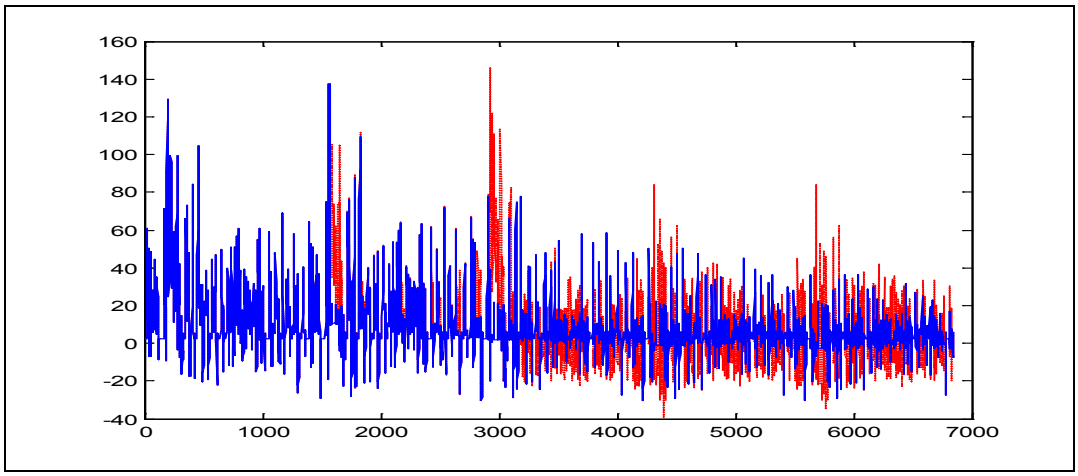

Figure 4.3 Current Drawn for Parallel Control Strategy (blue and continuous) and Current Drawn for Rule Based EMS (red and dotted) for Battery

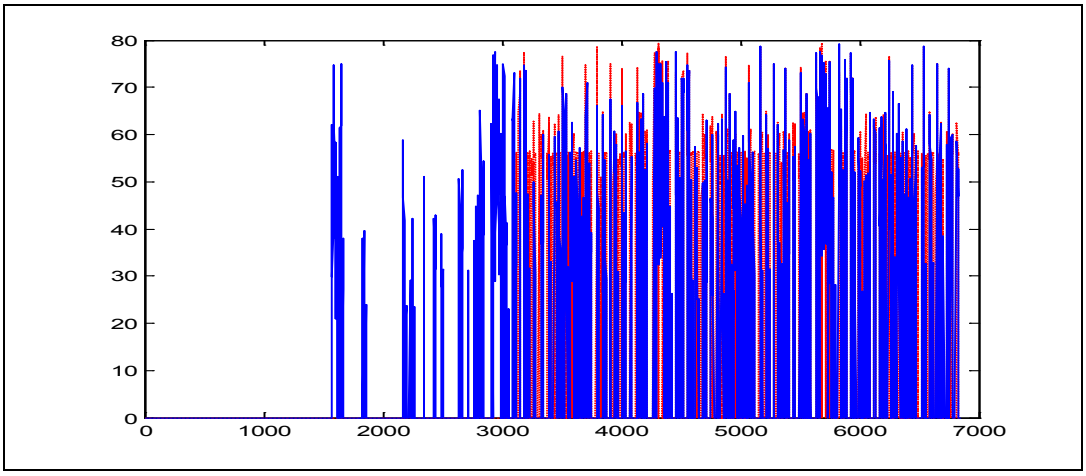

Figure 4.4 Engine Torque for Parallel Control Strategy (blue and continuous) and Engine Torque for Rule Based EMS

Figure 4.2 shows the SOC for the rule-based EMS when the vehicle made maximum use of the battery for first 3000 seconds compared to that for the parallel control strategy. But after that, the SOC was strictly maintained at the SOC Low value defined in the rule-based EMS strategy. The battery SOC is not allowed to go below this value so that the life time of the battery is not impacted by very deep discharge cycles.

Figure 4.3 reveals that ample current was drawn from and stored into the battery during the entire drive cycle for the Rule-Based EMS. But the amount of current drawn from and stored into the battery for the parallel control strategy was less compared to the rule based EMS. So the Rule-Based EMS made more use of the battery while it operated the engine near the efficient region during the drive cycle.

Figure 4.4 shows that the engine torque was maintained around the efficient operating region for most of the drive cycle, resulting in an increase in the engine efficiency which is validated by the engine efficiency values.

For these simulations on parallel powertrain the parallel control strategy provided 75.9 MPG while the rule-based EMS provided 80.9 MPG. During both the simulations the vehicle covered 37.3 miles of distance. Furthermore, the engine efficiency for the parallel control strategy was 28% but for the rule-Based strategy the engine efficiency was 29%. For the PHEV vehicle, Table 4.4 shows the MPG comparisons for different distances.

Table 4.4 MPG Comparison for Different Distances of Parallel Control Strategy and Rule Based EMS

No. of Drive Cycles (Distance in Miles)	3 (22.4)	5 (37.3)	7 (52.2)	10 (74.5)	15 (112)
Parallel control strategy MPG	124.6	74.6	62	54.3	48.4
Rule Based EMS MPG	194.2	80.9	64	55.5	50.4

Table 4.4 shows that the MPG results for Rule Based EMS always exceeded the parallel control strategy results. It is noted that MPG for the PHEV vehicle decreased as distance increased because as the distance increased the battery got discharged and the engine was used more. Furthermore, the starting SOC and the ending SOC for both the simulated strategies were the same. It can be concluded that MPG was improved by using Rule Based EMS.

4.1.2 Simulation for Powersplit Drivetrain

This section illustrates the simulation results for the Rule Based EMS with the powersplit drivetrain. Here the Rule Based EMS was simulated for a Powersplit drivetrain (Toyota Prius) and the results were compared with Prius default strategy in ADVISOR software. The Toyota Prius is a HEV with a powersplit drivetrain. This Prius can be modified into a Plug-in Hybrid Electric Vehicle by adding an additional battery pack and an external charging system to charge the battery from a domestic power supply.

A123 systems provide a battery pack system called the Hymotion L5 PCM. It is a Li-Ion battery pack with a maximum capacity of 5 kwh. This battery pack was installed in addition to the NiMh battery pack with a maximum capacity of 1.2 kwh. To simulate this battery pack a single Li-Ion battery pack of a maximum capacity of 6.3 kwh is used for the simulations. The Figure 4.5 shows a Prius PHEV which is modified from a Prius HEV by using an additional Hymotion L5 PCM battery pack.

Figure 4.5 Prius PHEV at Indiana University-Purdue University Indianapolis

The following sections include a simulation setup for the two strategies and their simulation results.

4.1.2.1 Simulation Setup

The simulation for the rule-based EMS for the powersplit drivetrain was implemented on the existing Toyota Prius vehicle model in ADVISOR. It was simulated for the converted PHEV vehicle by using larger battery pack. The energy capacity of the battery was redefined as 6.3 kwh. Moreover, it was assumed that battery was charged from an external domestic supply with 100% efficiency.

To implement the Rule Based EMS for a PHEV the same Prius powersplit drivetrain model was redesigned according to the requirements of the Rule Based EMS. Its various engine ON/OFF conditions were modified according to the characteristics of Rule Based EMS. Here the engine was operated at a selected speed which depended on the required power. The engine was also operated on maximum engine torque which was selected as an efficient operating region according to the strategy after analyzing the engine BSFC map. Thus the engine was being operated at specific speeds and torques. The models and the control parameters were initialized as mentioned in Table 4.5.

Table 4.5 Model and Parameter Values Used for Powersplit Powertrain with Rule Based EMS

Variable/Model	Value/Name
Engine	FC Prius JPN 57 kW
Motor	MC Prius JPN 50 kW
Battery	Li-Ion LI7
Max Battery Capacity	6.3 kwh
Initial Conditions	Hot Temp conditions
Init SOC	95%
SOC High	90%
SOC Low	35%

The details of the Prius control strategy are described in the appendix. To simulate the Prius control strategy in ADVISOR the following control parameters were defined.

Table 4.6 Models and Parameter Values Used for Powersplit Powertrain with Prius Control Strategy

Variable/Model	Value/Name
Engine	FC Prius JPN 57 kW
Motor	MC Prius JPN 50 kW
Battery	Li-Ion LI7
Max Battery Capacity	6.3 kwh
Initial Conditions	Hot Temp Conditions
Init SOC	95%
SOC High	90%
SOC Low	35%
Engine ON SOC	35%
Target SOC	45%
Engine ON Minimum Power Required	18,000 W
Electric Launch Speed Limit	34 MPH

4.1.2.2 Simulation Results and Analysis

Identical simulation models were used to implement both of the control strategies. Since one drive cycle cannot show a good comparison and the maximum capability of a PHEV, this vehicle was simulated for five drive cycles. The Prius powersplit powertrain was simulated for five consecutive UDDS drive cycles. The total distance travelled by vehicle was 37.2 miles. The vehicle speed attained while following the desired UDDS drive cycle is shown in Figure 4.6 below.

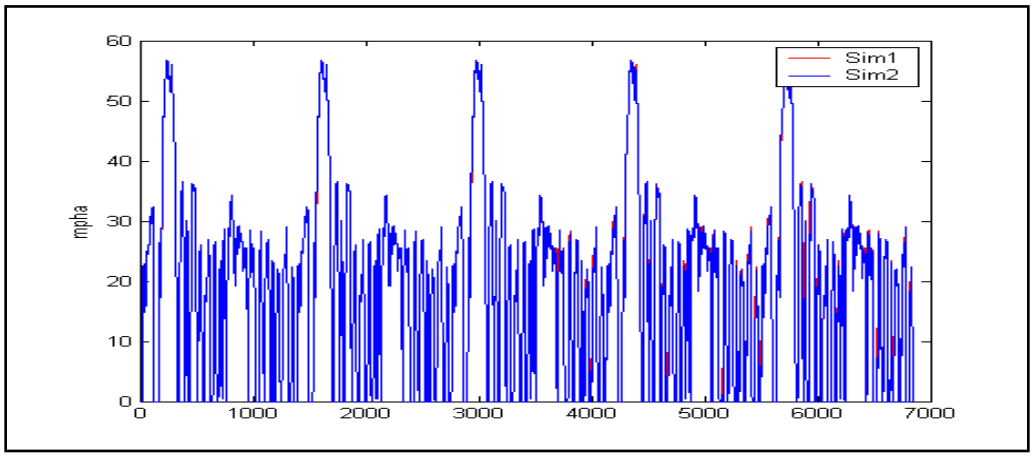

Figure 4.6 EPA Drive Cycle

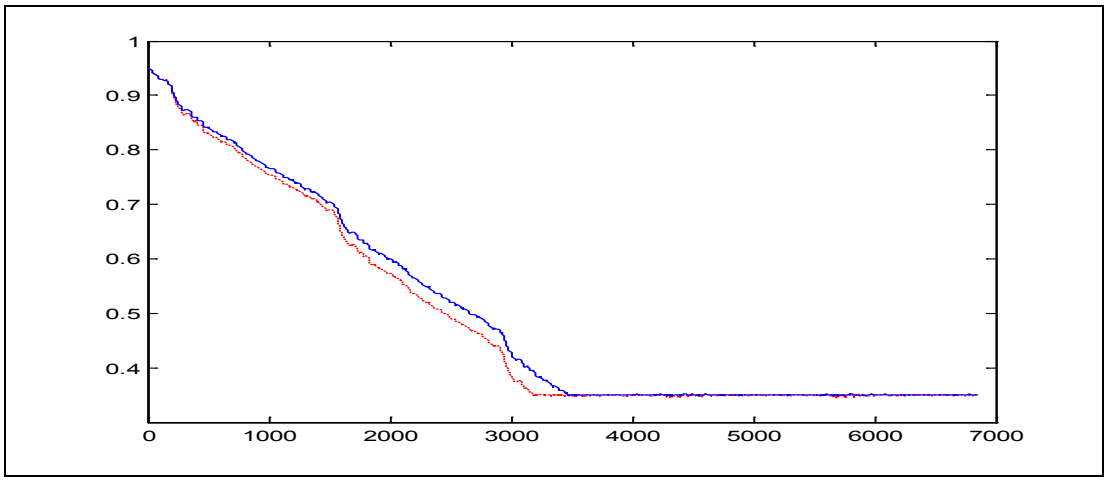

Figure 4.7 SOC of Prius Control Strategy (blue and continuous) and SOC of Rule based EMS (red and dotted)

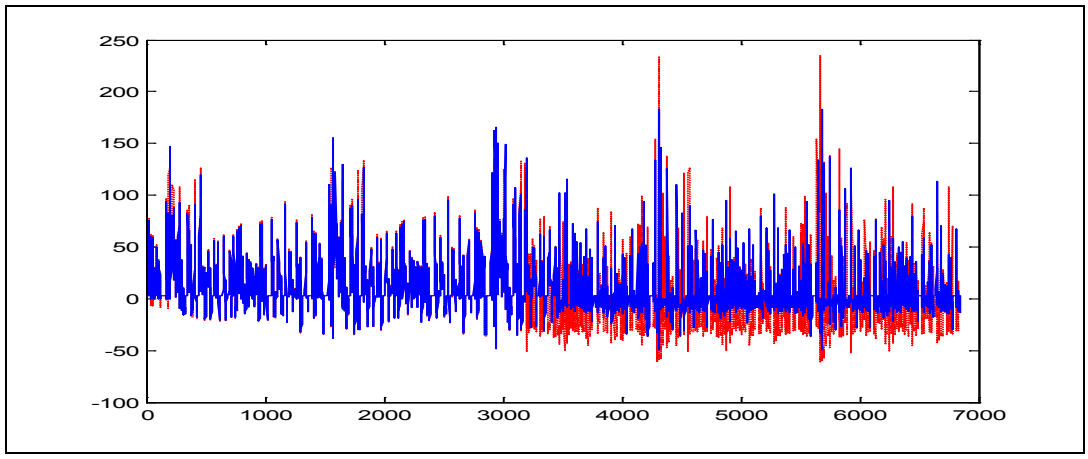

Figure 4.8 Current Drawn for Prius Control Strategy (blue and continuous) and Current Drawn for Rule based EMS

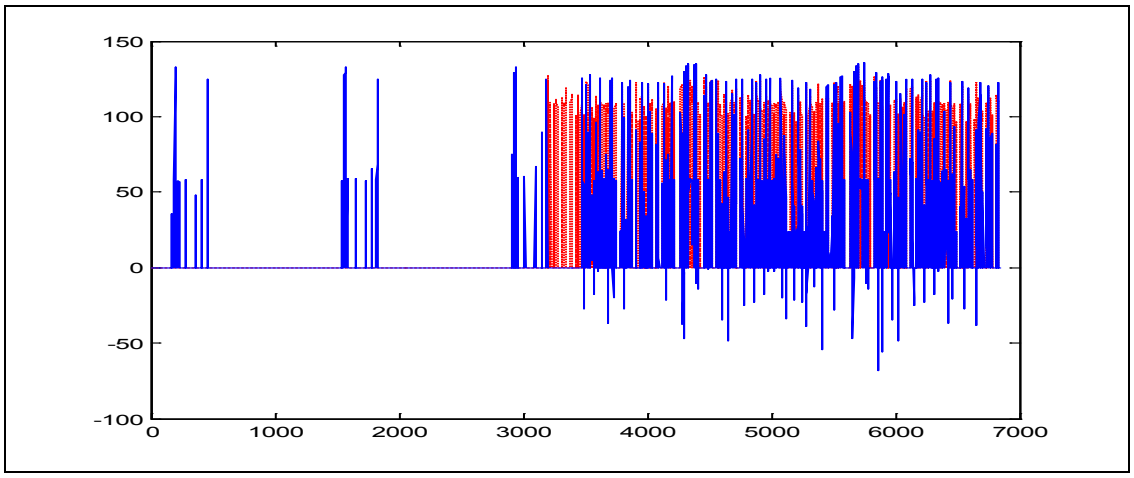

Figure 4.9 Engine Torque for Prius Control Strategy (blue and continuous) and Engine Torque for Rule Based EMS (red and dotted)

Figures 4.7 through 4.9 show the simulation results for SOC, battery current drawn and engine torque for both the Prius control strategy and the Rule Based EMS. Figure 4.7 shows that the rule-based EMS made maximum use of the battery for about 300 seconds compared to the Prius control strategy. After 3000 seconds both control strategies maintain the battery SOC near the SOC low which was defined in the parameters to be 30%. Both the control systems avoided the battery being depleted

further beyond this SOC to prevent any impact of deep discharge cycles of the battery on its life.

Figure 4.8 reveals that this rule-based EMS stored more charge into the battery compared to the Prius control strategy while operating the engine in an efficient region. From Figure 4.9 we can ascertain that the engine torque was mostly constant near the efficient operating region of the engine.

The Prius control strategy for PHEV powertrain showed gas mileage of 74.8 MPG, whereas the Rule Based EMS provided mileage of 87.6 for the drive cycle of 37.2 miles. Moreover the engine efficiency for the proposed RBS strategy on Prius model was increased to 35%. Since it is a PHEV vehicle better analysis can be attained by determining the vehicle MPG for different distances. This is shown in the table below.

Table 4.7 MPG Comparison for Different Distances of Prius Control Strategy and Rule Based EMS

No. of Drive cycles (Distance in Miles)	3 (22.4)	5 (37.4)	7 (52.2)	10 (74.5)	15 (112)
Prius control strategy MPG	202.9	74.8	59	51	45.9
Rule Based EMS	234	87.6	68.7	59.3	53.6

Table 4.7 shows that the Rule Based EMS always had better MPG results as compared to the Prius control strategy. It also shows that the MPG of PHEV decreased with increase in distance traveled by vehicle. Moreover, Figure 4.6 shows that the SOC

starting value and the ending value were the same for both of the control strategies. Hence it ascertains that the MPG of the vehicle improved by using Rule Based EMS.

4.2 Particle Swarm Optimized EMS Simulation

This section covers the simulation of the powersplit drivetrain vehicle when applying the Particle Swarm Optimized EMS. This EMS was only implemented on the powersplit drivetrain. Here the simulation software PSAT, a modeling tool developed by Argonne National Laboratory for hybrid and electric vehicles, was used. It is a forward-facing, simulation based vehicle modeling tool. It is used to simulate vehicle fuel economy and performance by taking into consideration the transient behavior and the different control system characteristics. It has a variety of different component models in its library which are derived from experimental results. These components can be used to build a desired vehicle drivetrain configuration and then can be simulated in the Matlab/Simulink based environment of PSAT.

In this simulation, PSAT was used to simulate the performance of the vehicle for different control strategies. The following section includes the simulation setup and the simulation results followed by analysis.

4.2.1 Simulation Setup

The constrained Optimization problem formulated in Section 3.2.1 was solved using the Particle Swarm algorithm as shown in the Figure 3.1. To implement this PSO algorithm a simplified model of the powersplit drivetrain was used as mentioned in Section 3.2.1. Then this simplified model was used to get the optimum operating points of the engine for the entire drive cycle. The optimum parameter values were evaluated after each second for the entire drive cycle. The results of this PSO which were near optimal operating points of the engine were then given to more complex PSAT model for better analysis and study. So the entire process of simulation was implemented as shown

in Figure 3.2. The simulation results were then compared with the PSAT control strategy.

For simulation the model was built in PSAT with the configuration described in Table 4.8 below:

Table 4.8 Model Components Details.

Component	Model
Generator	30 kW PM Motor
Energy Storage	6.3 kwh Li Ion Battery
Motor	50 kW PM Motor
Gearbox	Planetary Gear
Engine	57 kW Prius Engine

The same model components were used for both control strategies to provide legitimate comparisons of the control strategies. Both the control strategies were driven for UDDS drive cycles. The UDDS drive cycle was of 7.45 miles and 1367 seconds duration. Other characteristics of the UDDS drive cycle are given in Table 4.3.

The Figure below shows the Urban Dynamometer Drive Schedule (UDDS) drive cycle used for simulation.

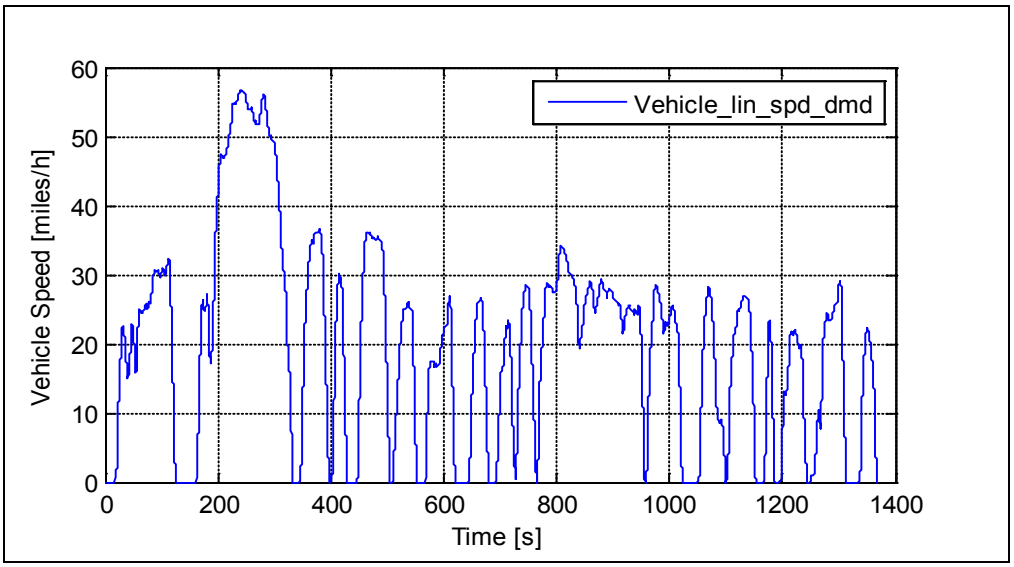

Figure 4.10 UDDS Drive cycle

4.2.2 Simulation Results and Analysis

In this simulation one drive cycle of UDDS as shown in Figure 4.10 was given as input to the model. For this given drive cycle the vehicle followed the drive cycle while satisfying the performance completely. Figure 4.11 shows the output vehicle speed attained by the vehicle while following the desired drive cycle shown in Figure 4.10.

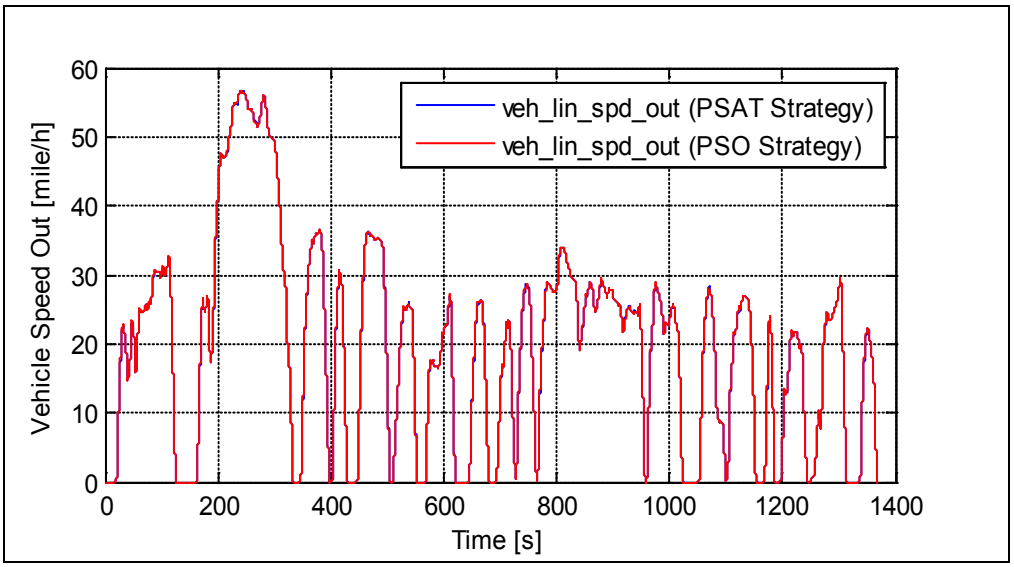

Figure 4.11 Vehicle Output Speed for PSAT and PSO Strategies

During the drive cycle the engine was operated at optimum operating points obtained from PSO for the PSO strategy.

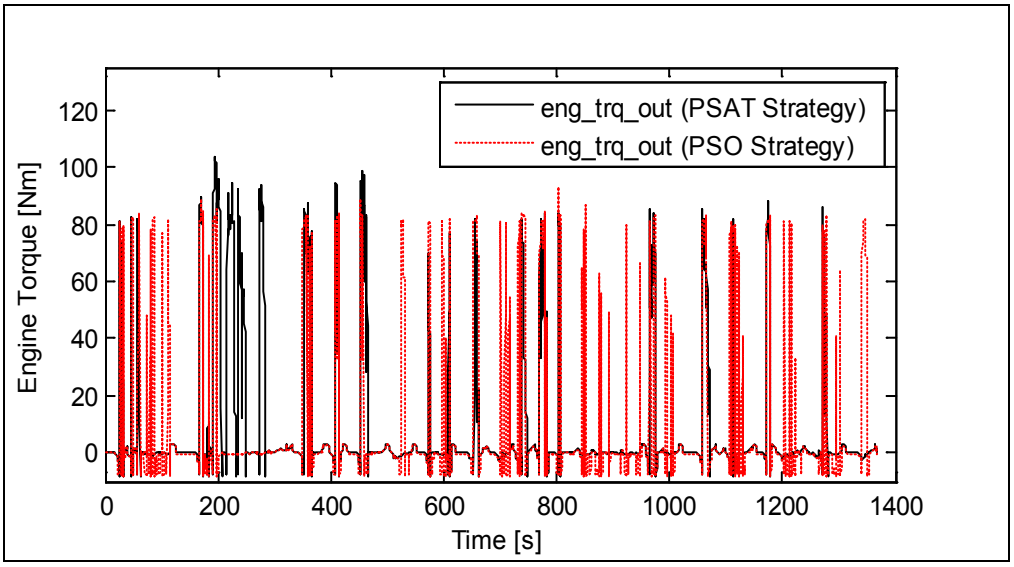

Figure 4.12 Engine Torque for PSAT and PSO Strategies

Figure 4.12 shows that the engine torque was consistently near the maximum engine torque which was in the more efficient operating region for the engine.

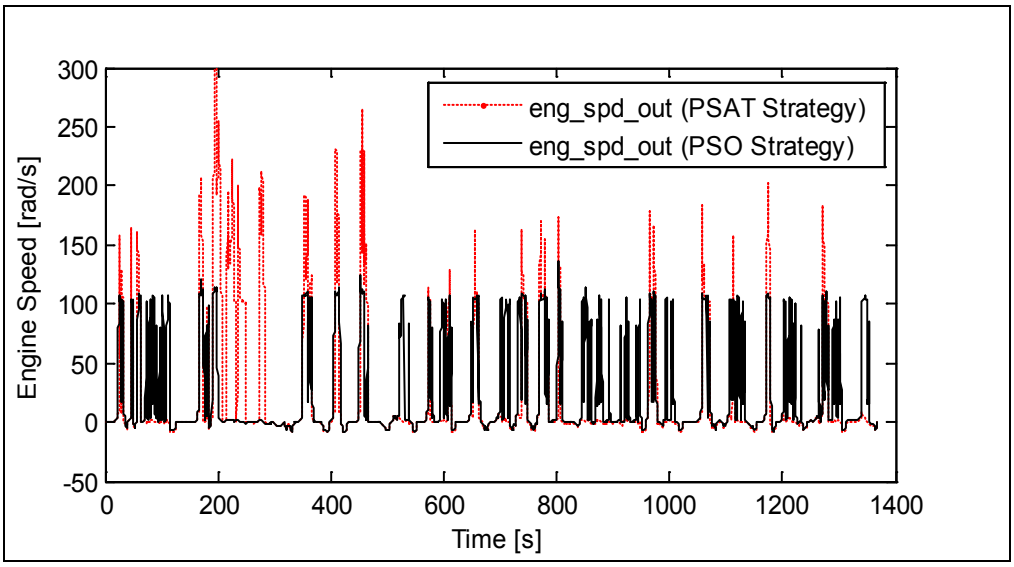

Figure 4.13 Engine Speed for PSAT and PSO Strategies

Figure 4.13 shows the engine's operating speed for both the PSAT and the PSO strategies. It can be seen that the engine was operating at lower speeds for the PSO strategy as compared to the PSAT strategy. The engine speed also had some negative values which occur while the engine is off. When the engine is off, the generator rotates because of planetary gear coupling. Therefore the engine is rotated at minor speeds of about 5 rad/sec in the reverse direction.

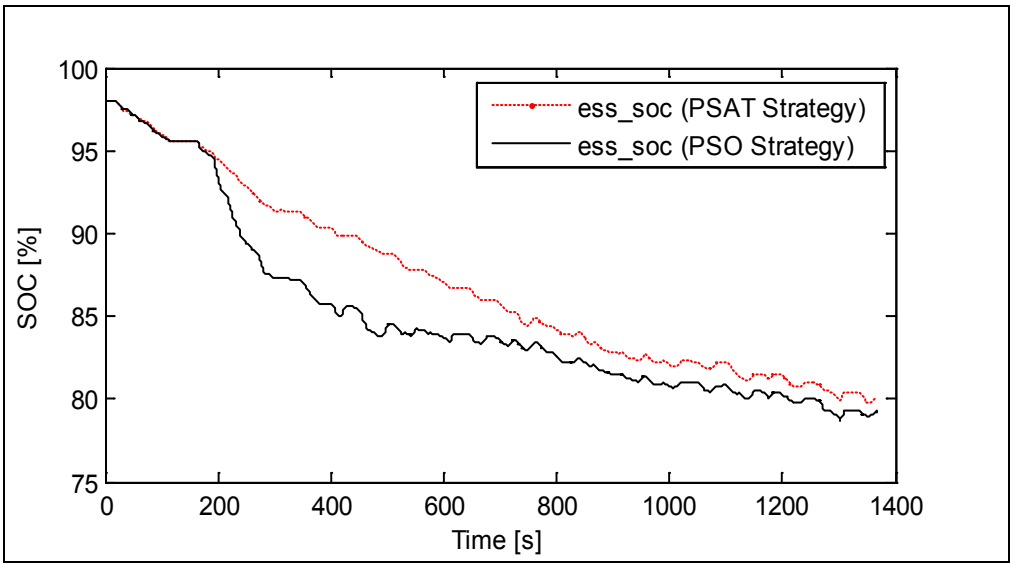

Figure 4.14 SOC of Battery for PSAT and PSO Strategies

Figure 4.14 shows the SOC of the battery for both strategies. Both the strategies had an initial SOC of 98%. At the ending the SOC is almost the same for both strategies with a minor difference of 0.75%. The SOC was depleted more for the PSAT strategy. Whereas SOC for the PSO strategy depletes very rapidly between 200 and 350 seconds because of the sharp demand of speed in the drive cycle between that period. But this SOC was almost maintained between 450 and 775 rad/sec because regenerative braking recovered the power and the engine provided the power to charge it.

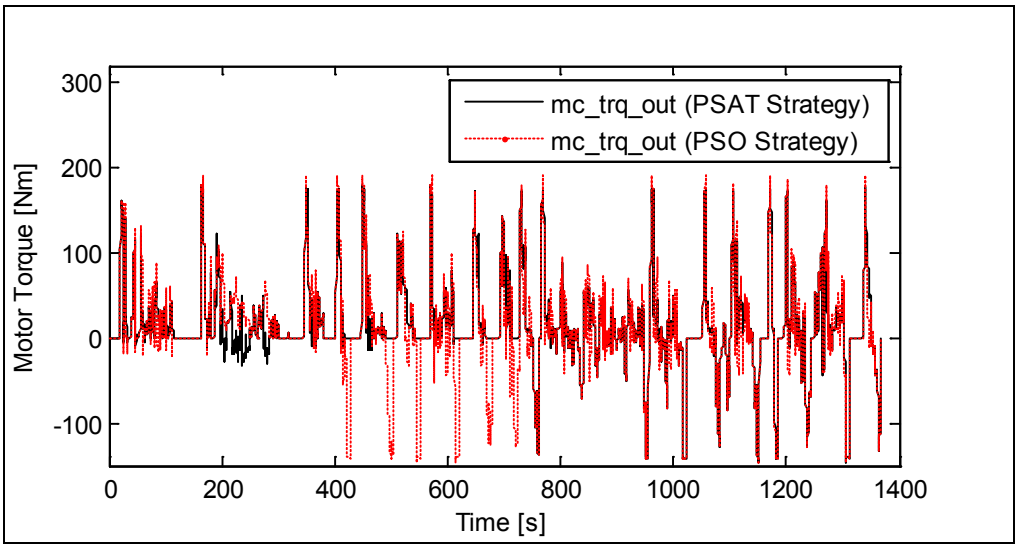

Figure 4.15 Motor Torque for PSAT and PSO Strategies

Figure 4.15 shows that the motor torque was more negative between 400 and 750 seconds of the drive cycle. Consequently, the battery current was also negative in Figure 4.16. Hence more regenerative energy was stored into the battery for the PSO strategy as compared to the PSAT strategy. In addition to the above results, between 200 and 350 seconds the current was more positive implying more amount of energy was used from the battery. Meanwhile the motor torque was more positive for the PSO strategy compared to the PSAT strategy for that duration. Hence, comparatively, the motor provided higher power at higher vehicle speeds to satisfy the positive power which the vehicle demanded for the PSO strategy.

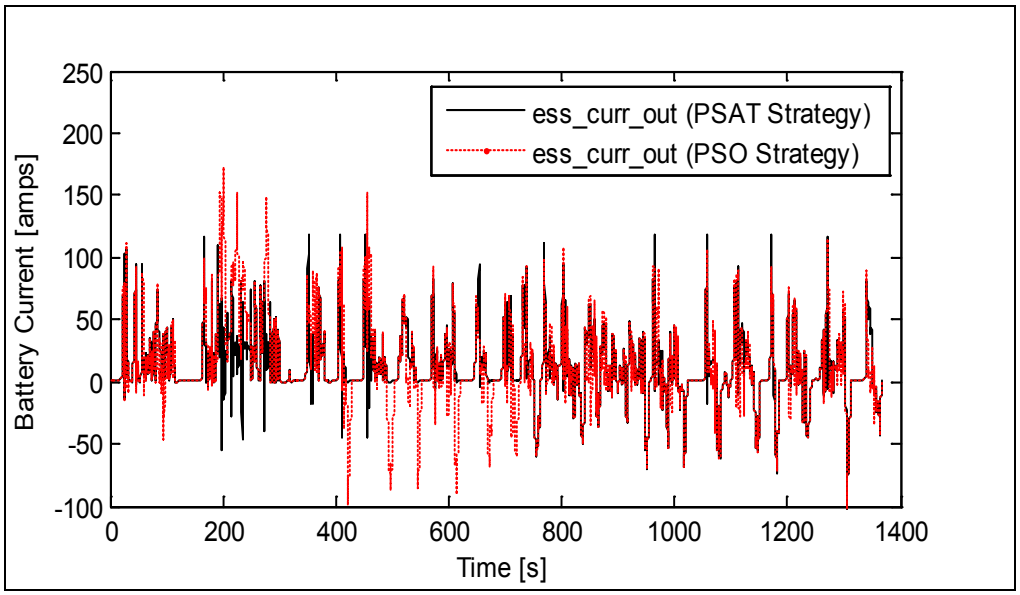

Figure 4.16 Battery Current for PSAT and PSO Strategies

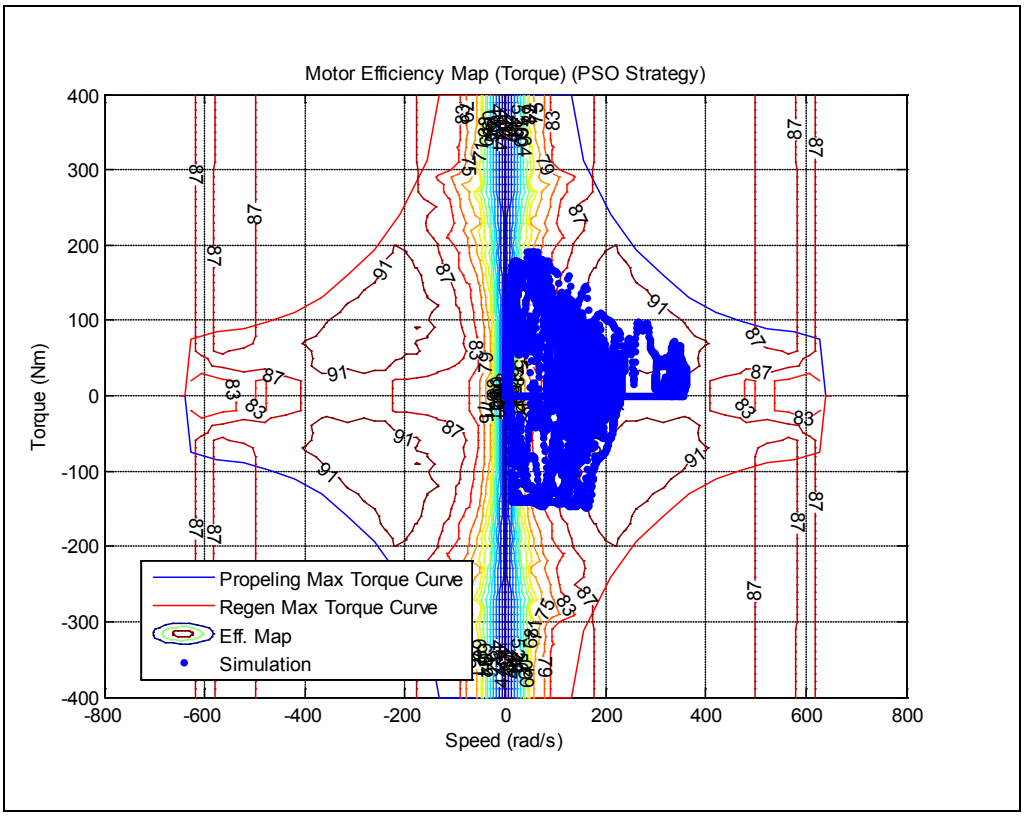

Figure 4.17 Motor Efficiency Map PSO Strategy

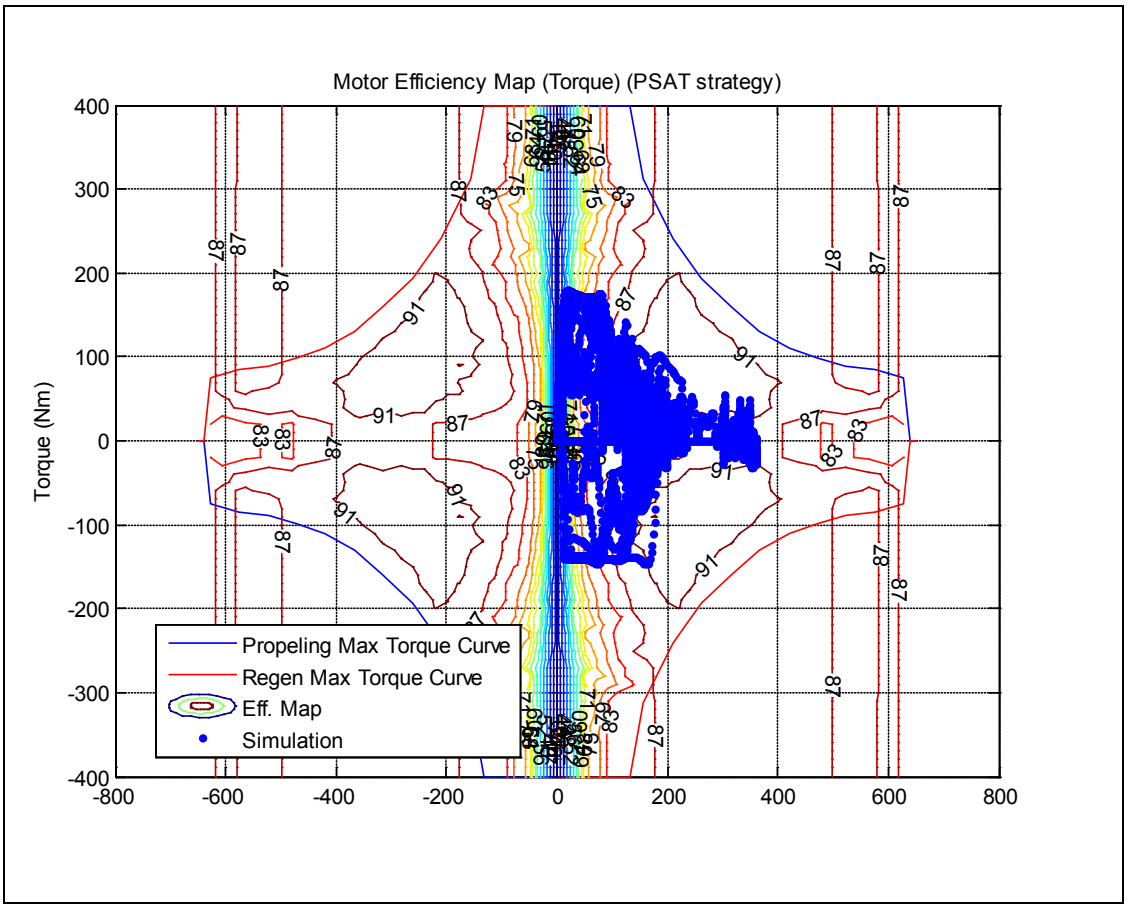

Figure 4.18 Motor Efficiency Map PSO Strategy

Figures 4.17 and 4.18 show the motor efficiency maps for both the PSAT strategy and the PSO strategy. By comparing the plots it can be seen that for the PSO strategy the Figure had more operating points in the efficiency region of about 91% in the first quadrant. It also shows that the motor efficiency increases marginally to 87.27% for the PSO strategy as compared to 86.43 % for the PSAT strategy.

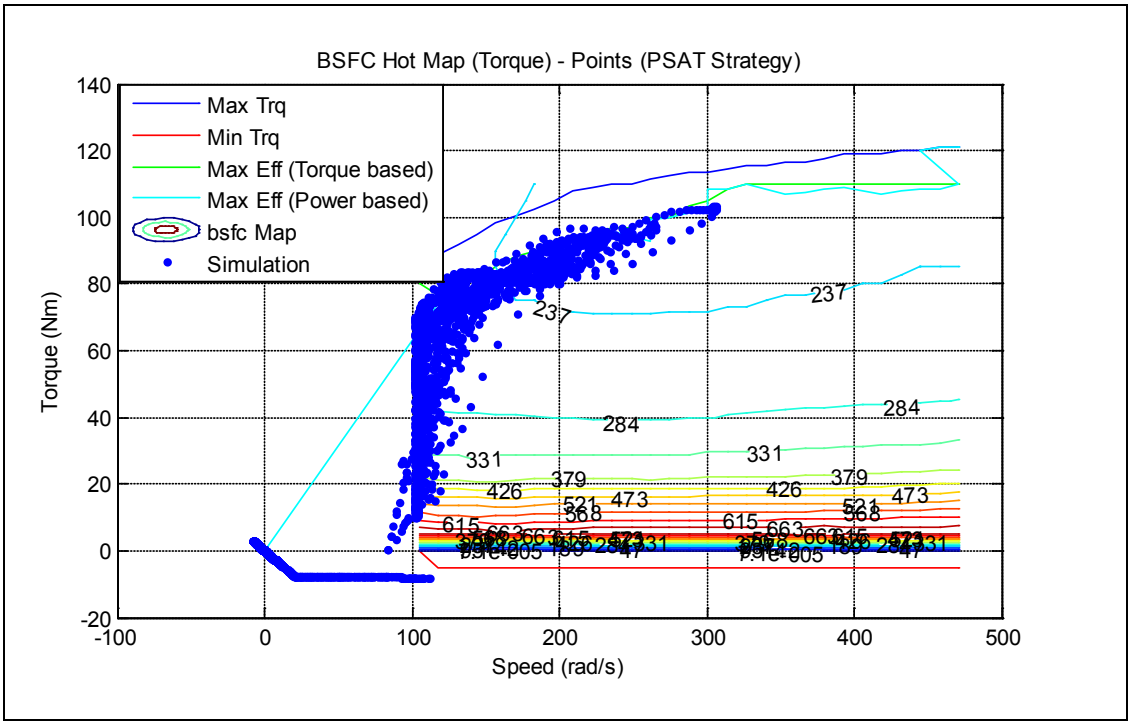

Figure 4.19 Engine BSFC Hot Map for PSAT Strategy

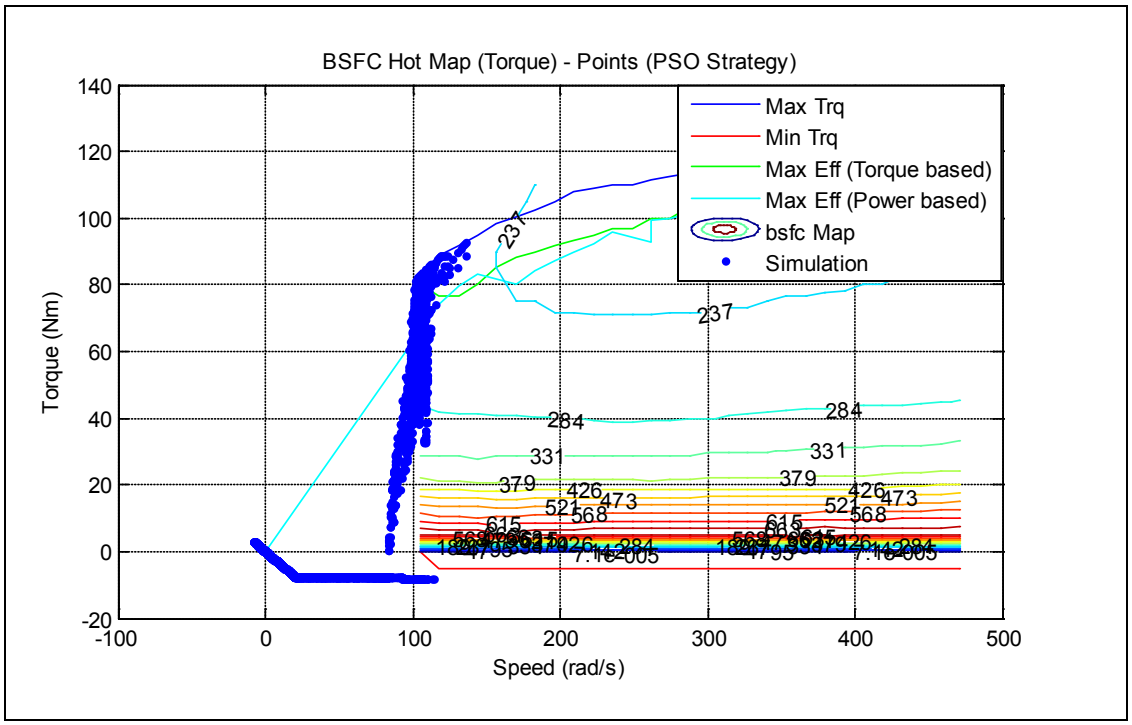

Figure 4.20 Engine BSFC Hot Map for PSO Strategy

Figures 4.19 and 4.20 show the engine BSFC Hot Maps for PSAT and PSO strategies respectively. The Figures show that for PSO strategy all the operating points are near the idle speed of the engine. It indicated that the fuel consumption was less. Meanwhile the performance of the vehicle was also satisfied. Moreover the engine torques and engine speeds were observed to be negative, because of the speed coupling that existed between the engine torque and the generator.

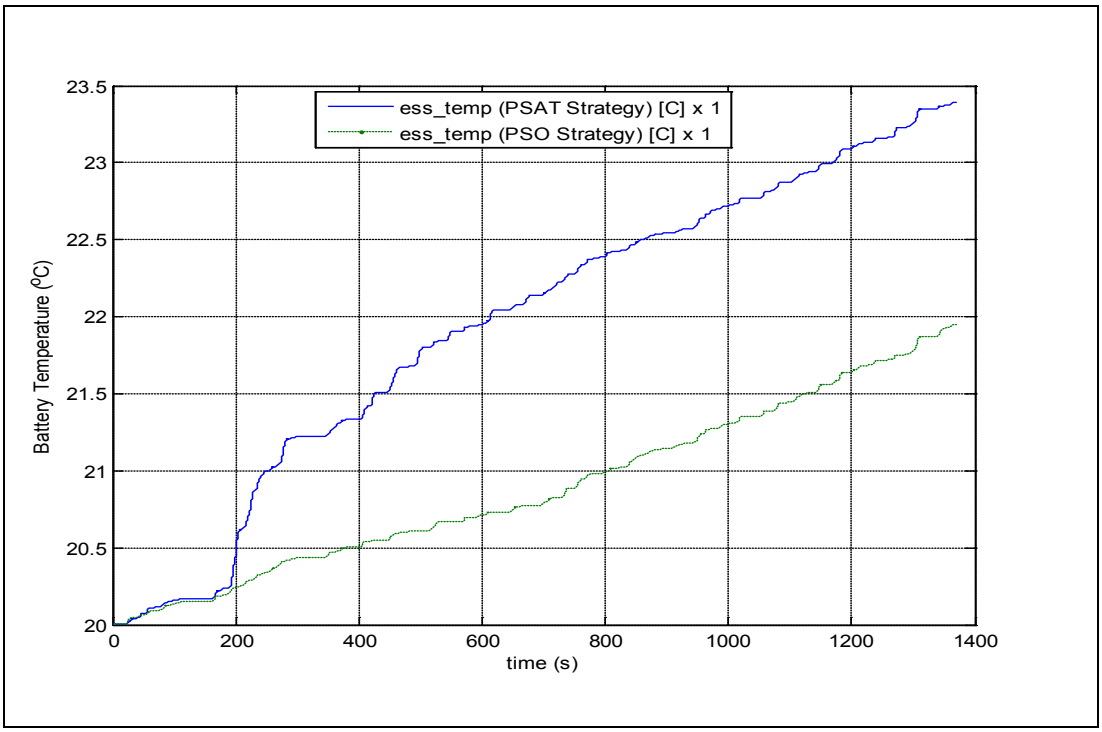

Figure 4.21 Battery Temperature for PSAT and PSO Strategies

Figure 4.21 shows that the battery temperature of the PSAT battery increased very sharply at 200 seconds because of the extra acceleration demanded by the drive cycle around that point. However, the battery temperature rise for the PSO strategy was rather steady in this simulation because the battery was used less for the PSO strategy as compared to the PSAT strategy.

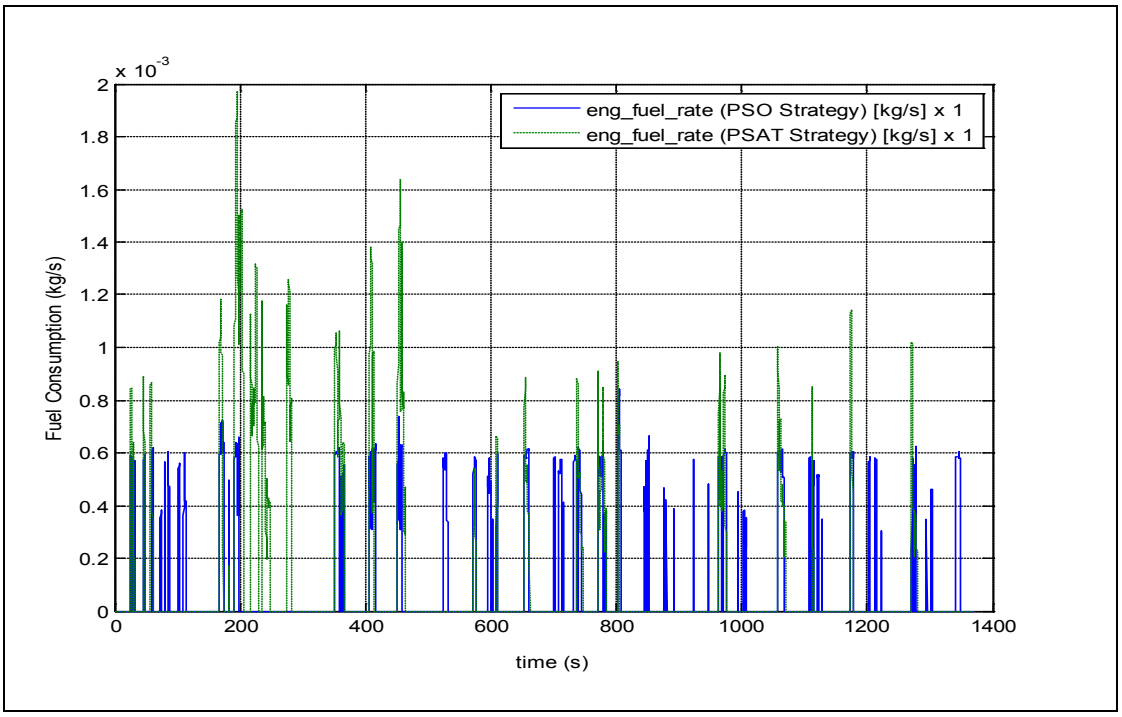

Figure 4.22 Fuel Consumption Rate by Engine for PSAT and PSO Strategies

Figure 4.22 shows the fuel consumption rate of gasoline in the engine for the PSAT and the PSO strategies. It can be clearly observed from the Figure that the fuel consumption rate for the PSO strategy was consistently less compared to the fuel consumption rate for the PSAT strategy because for the PSO strategy the engine was operated at lower speeds.

These simulation results are post processed by the PSAT software. The results of this post processed data are shown in Table 4.9. The results show higher mileage for the PSO EMS 192.8 miles/gallon as compared to 160.7 mile/gallon for PSAT strategy. Since the initial and final SOC values were the same for both the strategies the results are comparable.

Table 4.9 Simulation Post Processed Data Comparison for PSAT and PSO Strategy for One UDDS Drive Cycle

	PSAT Strategy	PSO Strategy	Unit
MPG	160.7	192/8	miles/gallon
Electrical consumption	114.64	119.10	Wh/mile
Mass of fuel to travel 320 miles	5.65	4.71	Kg
Powertrain bidirectional path Efficiency	49.53	53.72	%
Powertrain closed loop gain	0.73	0.8	-
Percentage energy recovered at battery	34.29	61.92	%
Absolute average difference on vehicle speeds	0.4	0.38	miles/hr
Absolute deviation from the trace	1.84	1.62	miles/hr

Both the strategies were blended mode strategies where both the engine and/or the battery can be used to power the vehicle, If the vehicle travels 320 miles distance on the same UDDS drive cycle the fuel consumption thus will be less for the PSO strategy compared to the PSAT strategy. The results show that the PSO strategy will have used only 4.71 Kg of fuel for 320 miles whereas PSAT strategy used 5.65 Kg of fuel, which is significant.

Table 4.9 shows that the overall bidirectional path efficiency for the PSO strategy was increased significantly to 53.72 % as compared with 49.52 percent for the PSAT

strategy. Similar results were observed for powertrain closed loop gain where it was increased to 0.8 for PSO strategy. Table 4.9 also shows that the percentage of energy recovered at the battery due to regeneration also increased notably to 61.92% as compared with 34.29% for the PSAT strategy. This fact was verified from the motor torque (Figure 4.14) and battery current (Figure 4.16) from simulation results between 400 and 800 seconds where large negative torques and negative currents were recovered and stored in the battery. In the same table, the comparison of absolute average difference between the vehicle's output speed and demanded drive speed was calculated. It also showed that the performance of vehicle was improved for the PSO strategy compared to the PSAT strategy.

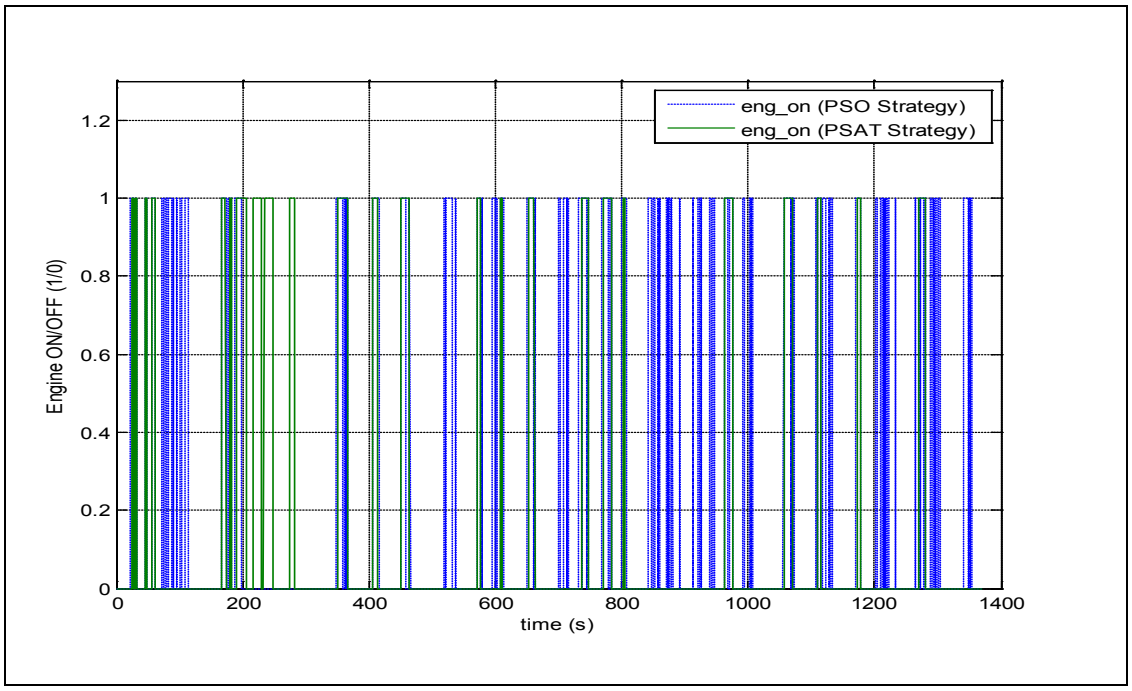

Figure 4.23 Engine ON/OFF for PSAT and PSO Strategies

Figure 4.23 shows the engine ON/OFF activity during the entire drive cycle for the PSAT and PSO strategy. Values of 1 indicate engine ON and values of 0 indicate engine OFF. The Figure shows that for the PSO strategy the engine turning ON/OFF is more frequently as compared to the PSAT strategy, which is less practical. So to avoid such

frequent engine transition an updated PSO optimized strategy was implemented which is described in Section 4.3.

4.3 Advanced Optimized EMS using PSO

This section includes the simulation of the powersplit drivetrain vehicle after applying the advanced optimized EMS using PSO. The powersplit drivetrain model from PSAT was used to simulate the vehicle.

The following section includes the simulation setup and the simulation results followed by its analysis.

4.3.1 Simulation Setup

The problem formulated for advanced PSO EMS described in Section 3.3.1 was solved using the PSO algorithm shown in Figure 3.1. It was simulated similar to the process used in Section 4.2. First, a simplified model of powersplit was used that was the same as the simplified model used in Section 4.2 developed using the modeling equations of Chapter 2. Second, this simplified model was used with the PSO algorithm which provided the optimum operating points of the engine for the entire drive cycle. Finally, the optimum results obtained from the second step were used in the simulation of the powersplit drivetrain in the PSAT as shown in Figure 3.2 for accurate modeling and easy analysis. The simulation results were compared with different control strategies.

The constrained optimization problem formulated in Section 3.3.1 was solved using the particle swarm algorithm as shown in Figure 3.1. To implement this PSO algorithm a simplified model of powersplit drivetrain was developed using the modeling equations described in the Chapter 2 for each component as mentioned in Section 3.2.1. Then, this simplified model was used to get the optimum operating points of the engine for the entire drive cycle. The near optimum parameter values of the engine speed and the

engine torque were evaluated after each second of the duration of the drive cycle. The results of this PSO, which were optimum operating points of the engine, were then given to more complex PSAT model for better analysis and study. So the entire process of simulation was implemented as shown in Figure 3.2. The simulation results were then compared with a PSAT control strategy, and results of the PSO EMS obtained in Section 4.2.

To compare the PSO EMS results with the PSAT control strategy and the advanced PSO EMS, the results obtained in Section 4.2 are extended to three UDDS drive cycles. This extension is valid because for the second and third drive cycle the power demands would be the same as that of the first drive cycle since the drive cycle is the same. Furthermore, even the SOC does not have any effect on the objective function since the difference in SOC is considered for the objective function evaluation. Moreover, for the UDDS drive cycle, the battery power charge/discharge limit curve showed that constraint Equation 3.15 is always satisfied for the battery operating power demands in the first drive cycle. Therefore, the PSO EMS results of the first drive cycle can be extended to the second and the third drive cycles and the comparison can be made to the other two strategies.

The simulation model was built in PSAT similarly as mentioned in Section 4.2.1. More details regarding the simulation are given in Table 4.8.

The same models were used for all the control strategies to have valid comparisons of the control strategies. All the control strategies were driven for three UDDS drive cycles. The total driving distance is 22.35 miles and time duration is 4109 seconds. Detailed characteristics regarding the UDDS drive cycle are given in Table 4.3.

4.3.2 Simulation Results and Analysis

As mentioned above the simulation was completed for three continuous UDDS drive cycles which are shown in Figure 4.24. For these three drive cycles the vehicle followed the 22.35 miles of distance for three UDDS drive cycles. The vehicle followed the drive cycle while satisfying the performance completely. The Figure shows the output vehicle speed attained by the vehicle while following the desired drive cycle as shown in Figure.

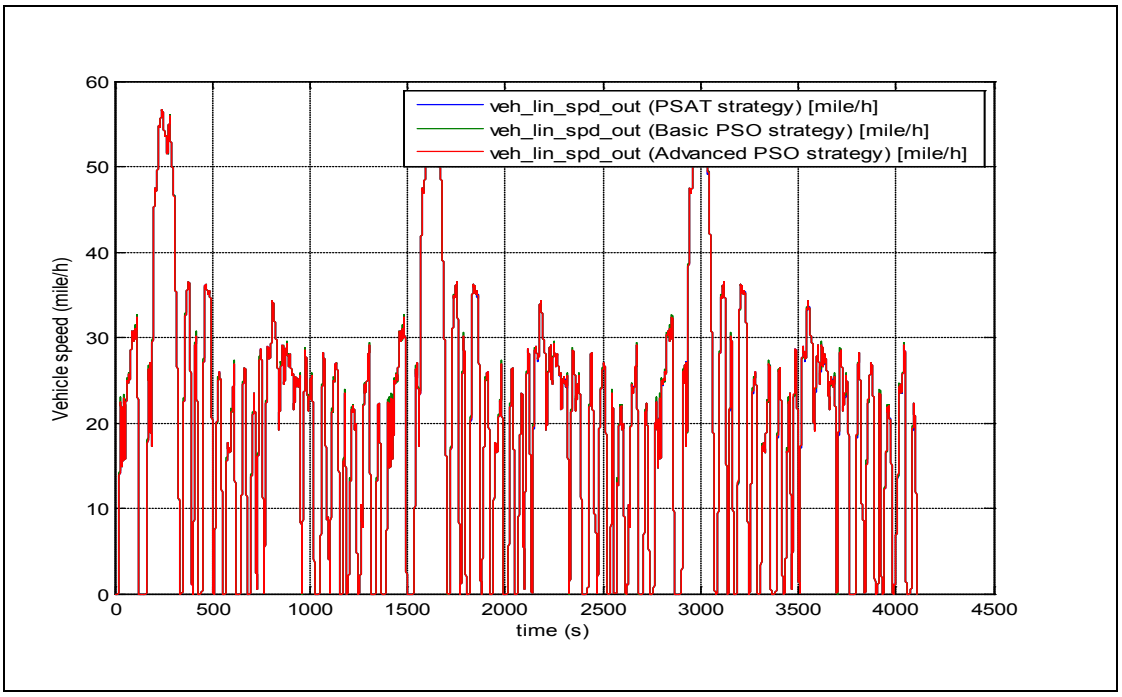

Figure 4.24 Vehicle Speed Attained for PSAT, Basic PSO and Advanced PSO Strategies

For basic and advanced PSO strategies the engine was operated at near optimum operating speeds and torques which were obtained from the PSO algorithm defined in Chapter 3.

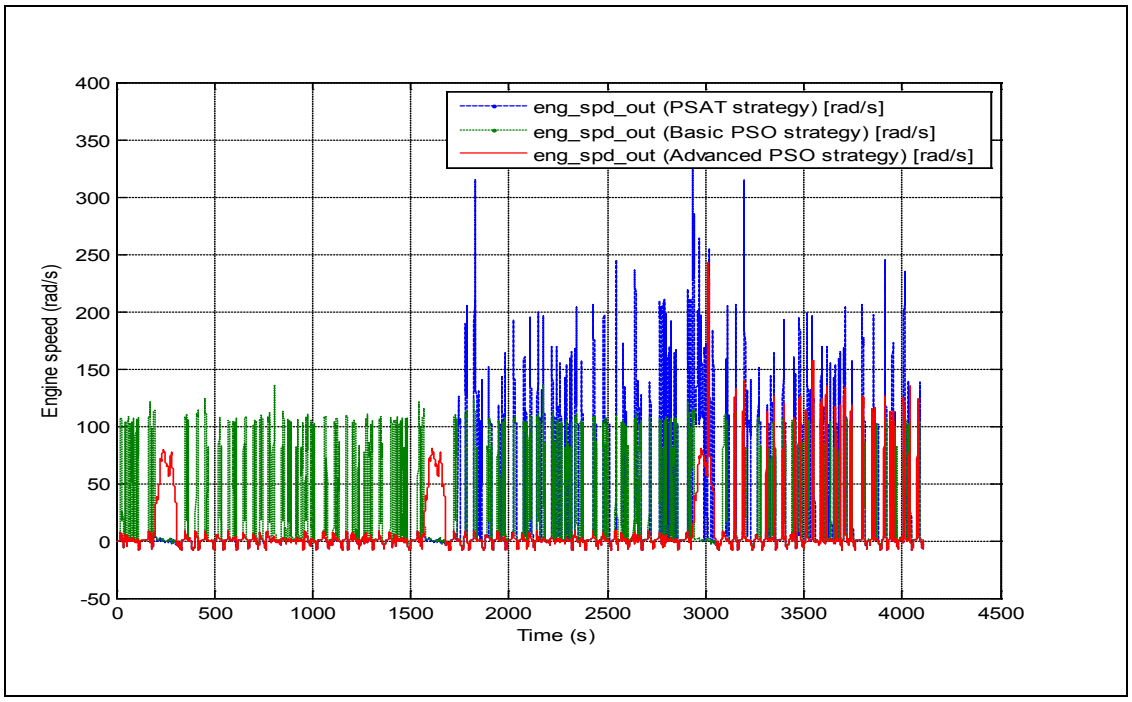

Figure 4.25 Engine Output Speed for PSAT, Basic PSO and Advanced PSO Strategies

Figure 4.25 shows the engine speeds for the PSAT strategy, basic PSO strategy and advanced PSO strategy. For the basic PSO strategy the engine was operated from the beginning of the UDDS drive cycle since those were the optimal engine speeds obtained from the PSO algorithm where the objective function considered the equivalent fuel consumption consisting of SOC and fuel consumption in its calculations. Moreover the engine was operated at optimum points. For the advanced PSO strategy it was seen that the engine was operated at higher speeds relative to the operating speeds of Basic PSO since it was operated less frequently, whereas the operating speeds for the PSAT strategy were very high.

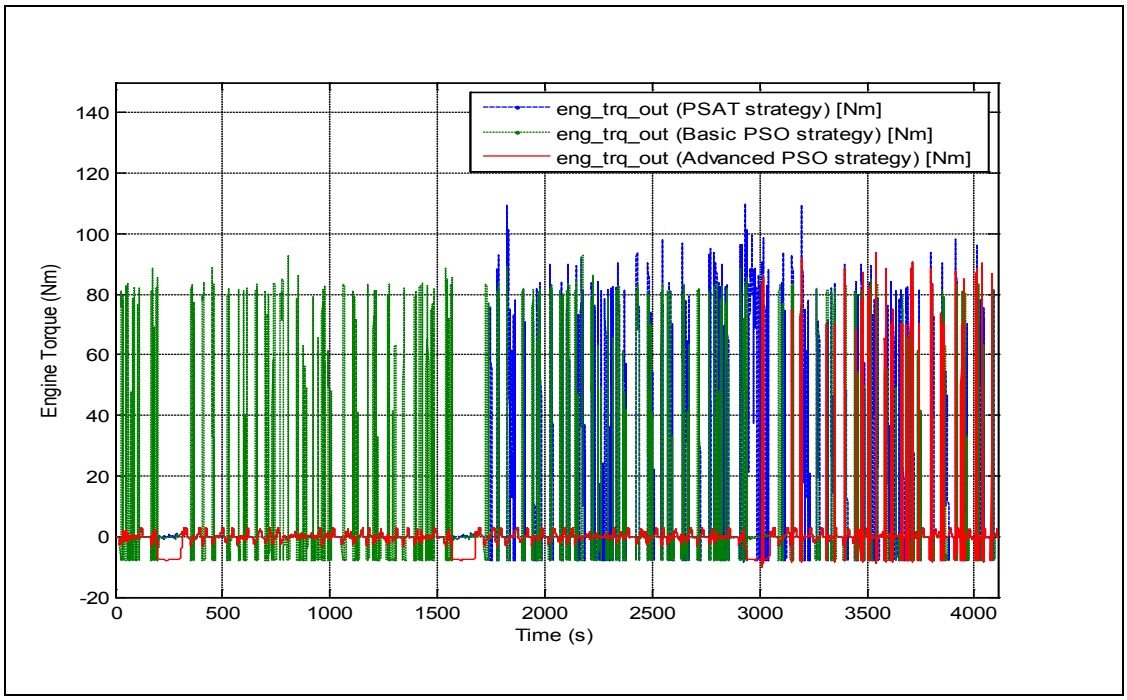

Figure 4.26 Engine Output Torques for PSAT Strategy, Basic PSO Strategy and Advanced PSO Strategy

Figure 4.26 shows the engine output speeds for the PSAT strategy, basic PSO EMS and advanced PSO EMS. The engine torques for Basic PSO EMS and advanced PSO EMS were obtained from the near optimum engine torque which were results obtained from PSO. The PSAT strategy engine torques were higher than the other EMS torques.

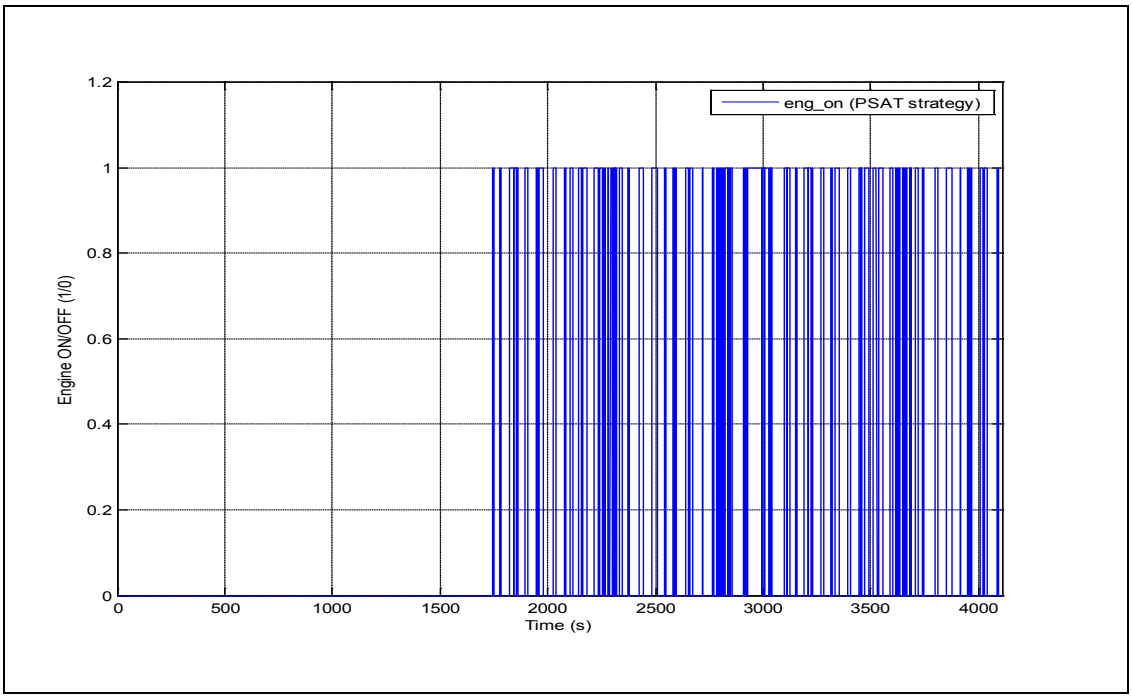

Figure 4.27 Engine ON/OFF for PSAT Strategy

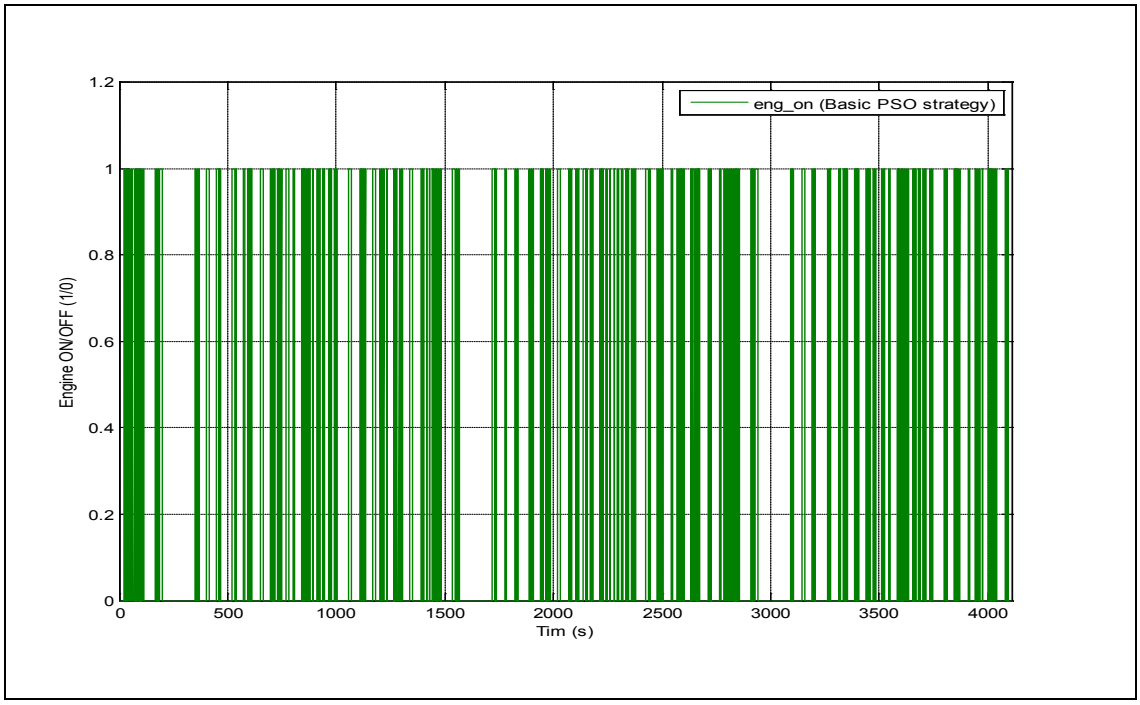

Figure 4.28 Engine ON/OFF for Basic PSO Strategy

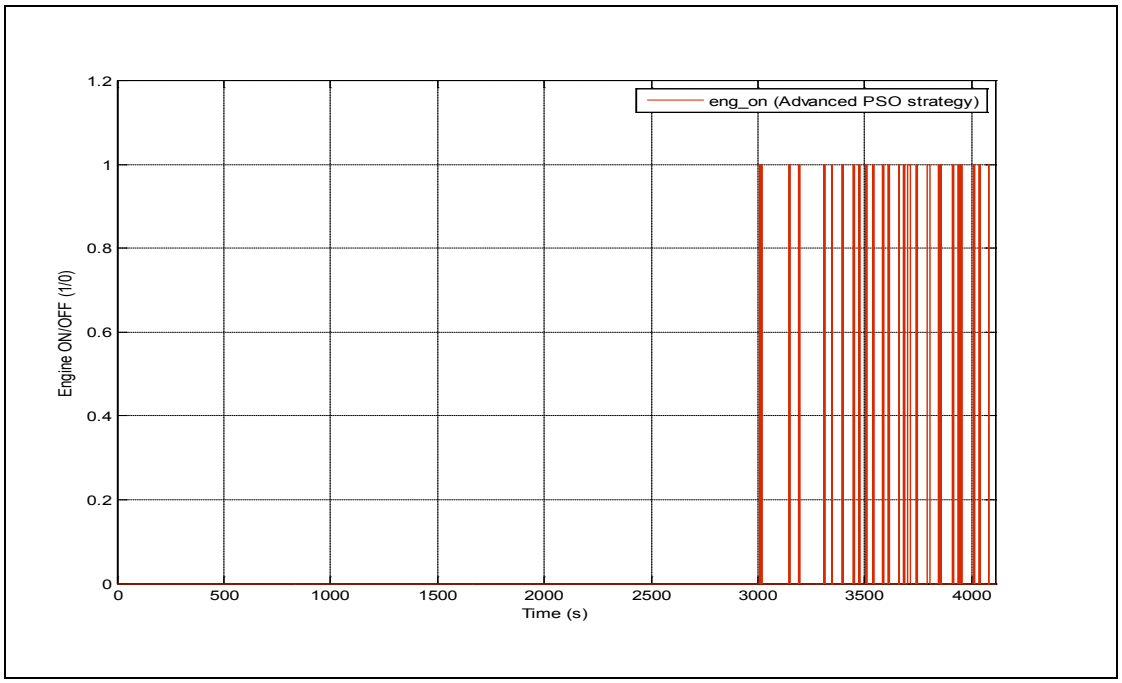

Figure 4.29 Engine ON/OFF for Advanced PSO Strategy

Figures 4.27 – 4.29 show the engine ON/OFF events for PSAT strategy, basic PSO EMS and advanced PSO EMS respectively. It was observed from the plots that the engine ON/OFF frequency was significantly reduced for the advanced PSO EMS as compared to Basic PSO EMS and the PSAT strategy. This engine ON/OFF frequency made the control strategy more practical and implementable on the vehicle.

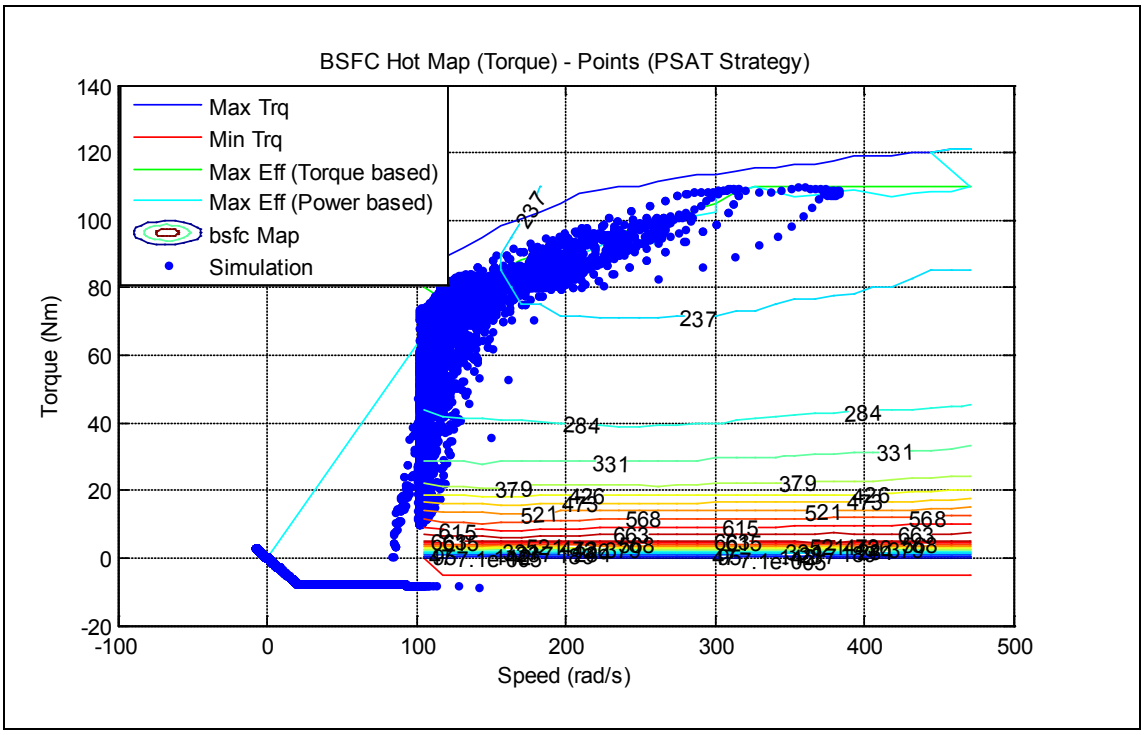

Figure 4.30 Engine BSFC Hot Map for PSAT Strategy

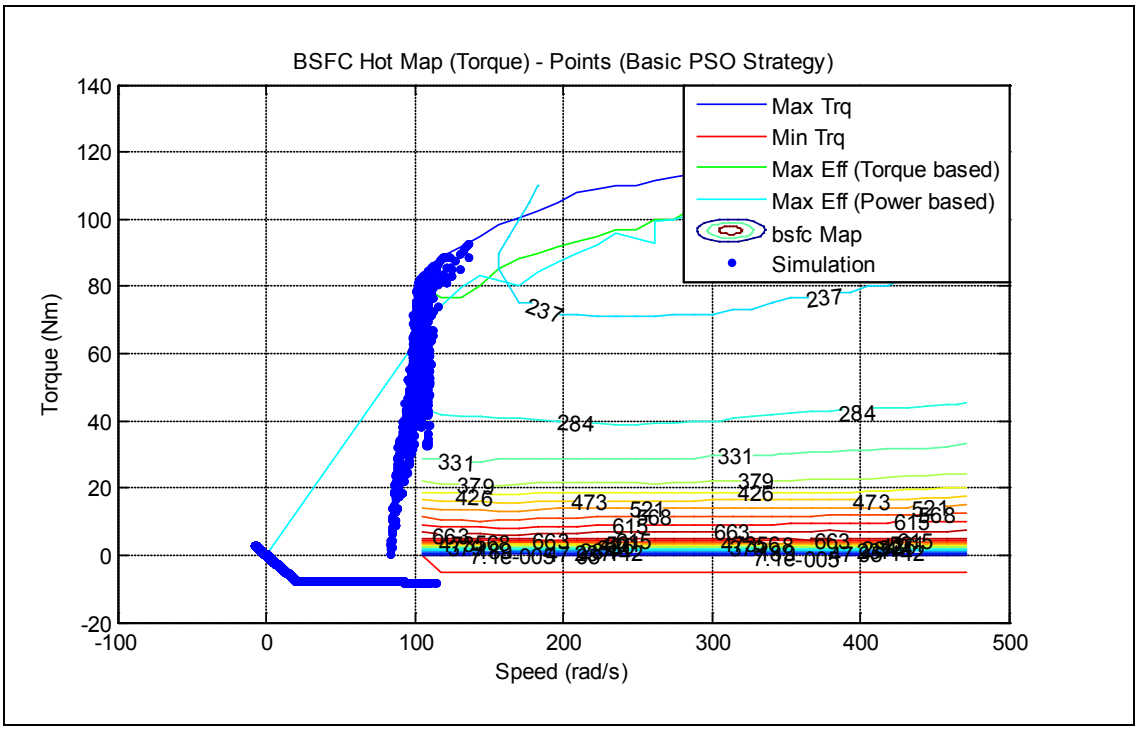

Figure 4.31 Engine BSFC Hot Map for Basic PSO Strategy

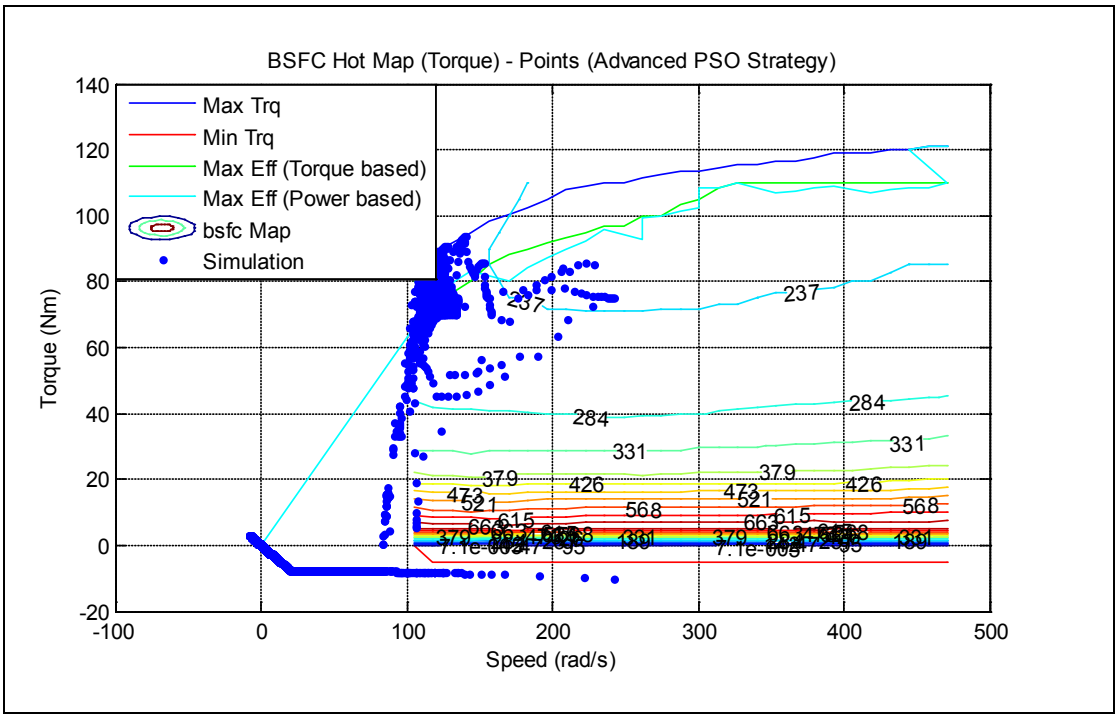

Figure 4.32 Engine BSFC Hot Map for Advanced PSO Strategy

Figures 4.30-4.32 show the engine BSFC map for the PSAT strategy, basic PSO EMS and advanced PSO EMS. The results of advanced PSO EMS show improvement in terms of fuel consumption over the PSAT EMS. Moreover, as compared to the basic PSO EMS some optimum operating speeds were farther away from the idle operating speed of the engine since it was operated less frequently so required more power to charge the battery during the third drive cycle.

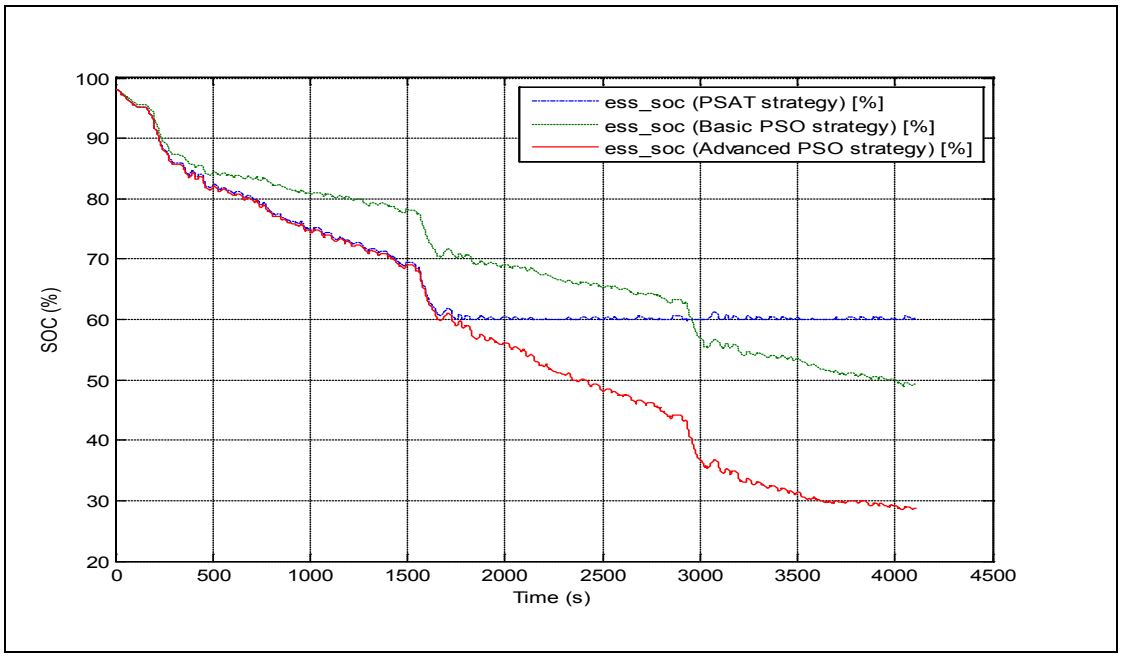

Figure 4.33 SOC of Battery for PSAT Strategy, Basic PSO Strategy and Advanced PSO Strategy

Figure 4.33 shows the SOC of battery for PSAT strategy, basic PSO EMS and advanced PSO EMS. The SOC curve for the advanced PSO strategy decreased more rapidly as compared to the Basic PSO EMS curve during the entire drive cycle. Until 1600 sec the SOC of the PSAT strategy and the advanced PSO EMS were depleted almost the same since they are running almost on EV mode. In the end the advanced PSO strategy SOC of the battery should have ended at 30 % but it ended at 28%. This was because of the approximation error between the simplified model used in optimization and the PSAT model used for analysis.

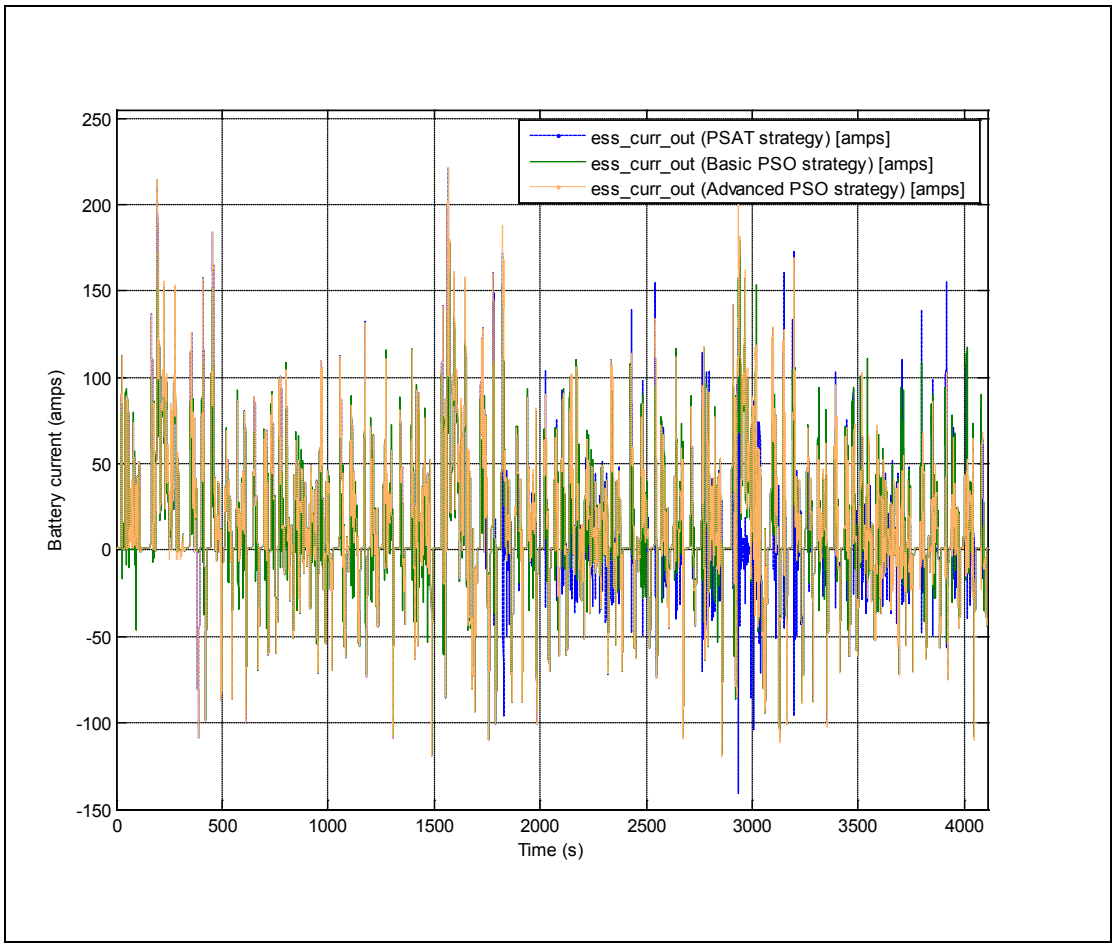

Figure 4.34 Battery Current for PSAT Strategy, Basic PSO Strategy and Advanced PSO Strategy

Figure 4.34 shows the battery current for all three strategies, i.e., PSAT strategy, basic PSO EMS and advanced PSO EMS. It clearly shows that large amount of currents were drawn from battery for advanced PSO EMS initially for 0 to 1600 seconds as it was used to drive the vehicle. Moreover, for time from 0 to 350 seconds there were no negative currents because the battery was fully charged during that time interval and it did not require charging from the engine.

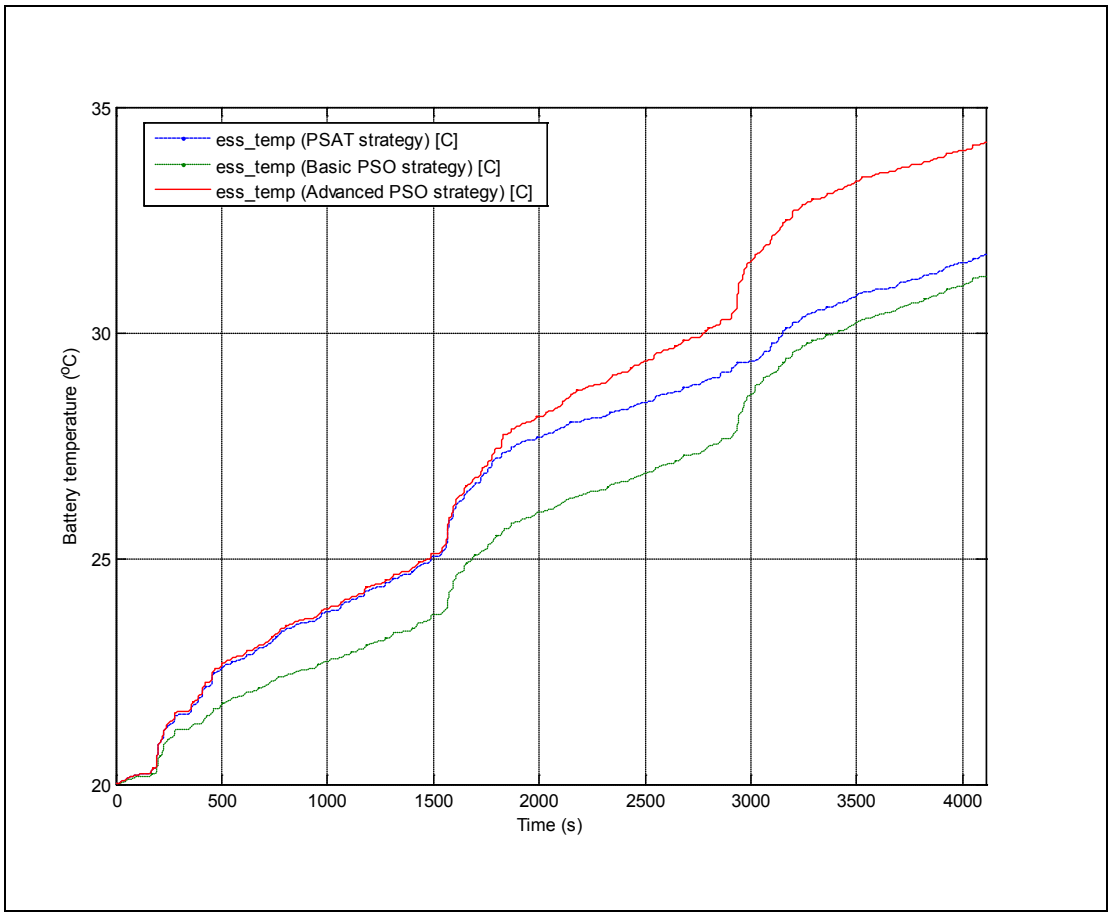

Figure 4.35 Battery Temperatures for PSAT Strategy, Basic PSO Strategy and Advanced PSO Strategy

Figure 4.35 shows the battery temperatures for three different strategies. As shown it clearly shows that the battery temperatures for the advanced PSO strategy were much higher. So it required a better battery cooling system to maintain the battery at the desired temperature. The battery temperature control system is not incorporated into the simulation model hence the energy required for the cooling system is assumed to be zero.

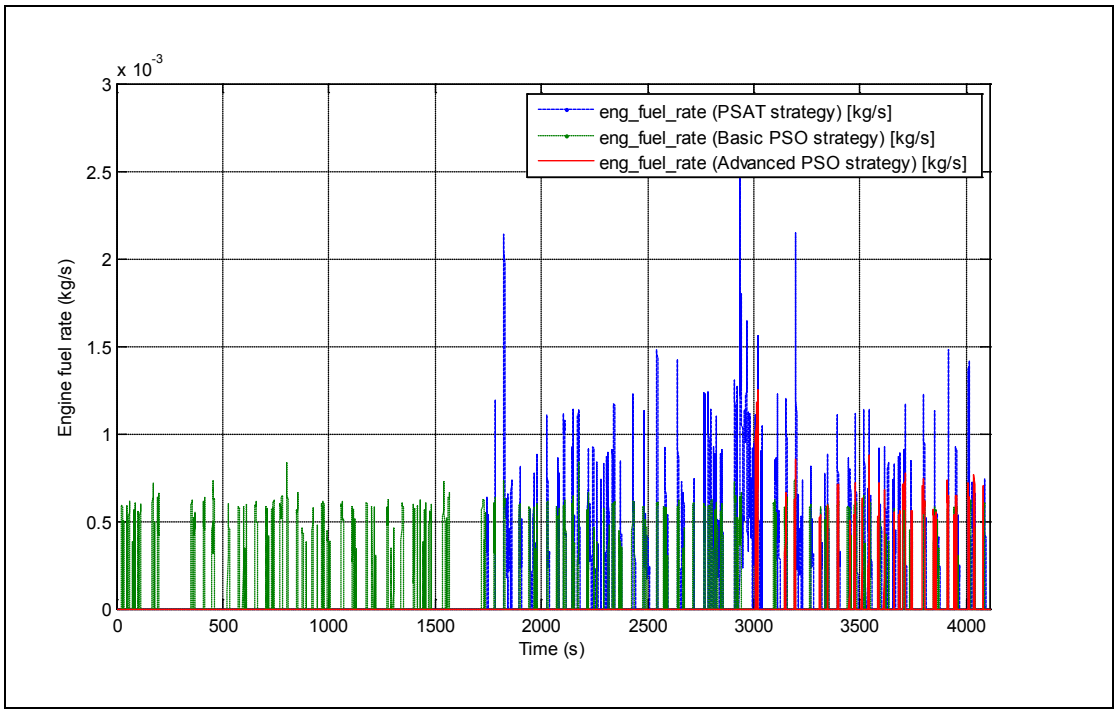

Figure 4.36 Instantaneous Fuel Consumption for PSAT Strategy, Basic PSO Strategy and Advanced PSO Strategy

Figure 4.36 shows fuel consumption by the engine for time intervals of 1 second. It shows that the fuel consumption values for the basic PSO strategy and the advanced PSO EMS which were near optimal results were smaller compared to the PSAT strategy values. Moreover it also shows that the values of fuel consumption for the advanced PSO were 0 until 3000 seconds since engine was not turned on. But when it was turned on its values were relatively larger than basic PSO EMS since the engine was providing more power during that time interval.

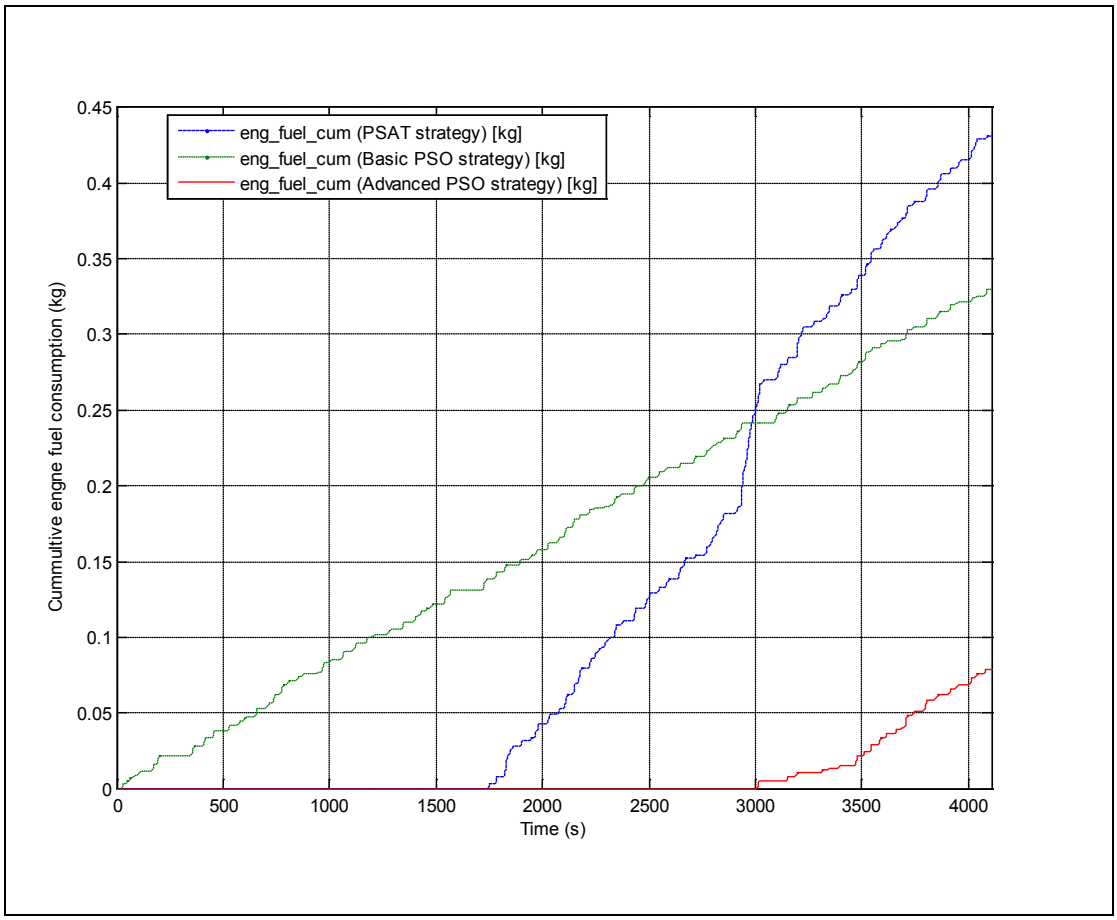

Figure 4.37 Cumulative Fuel Consumption for PSAT Strategy, Basic PSO Strategy and PSAT Strategy

Figure 4.37 shows that fuel consumption for the basic PSO strategy was consistent throughout the drive cycle since it was based on optimum results of PSO for the objective function using equivalent fuel consumption for calculations. Moreover the PSAT strategy was in EV mode for 0 to 1700 seconds but after that it started using engine and consumed fuel very rapidly. The cumulative fuel consumption curve for the advanced PSO EMS shows that until 3000 seconds it used almost no fuel as it was running on EV mode and the battery was driving the vehicle. But afterwards it started consuming the fuel but at faster rates. The advanced PSO EMS problem was formulated such that initially the vehicle is running in EV mode while consuming battery but afterwards it uses

the engine to maintain SOC around a certain value to avoid further depletion and harm to the battery life.

Figure 4.36 shows three kinds of strategies. They are blended mode strategy which was basic PSO EMS, charge sustaining and charge depletion strategy which was not optimized i.e. PSAT strategy and optimized advanced PSO EMS.

Table 4.10 Summary of Comparisons among Different Strategies

	PSAT	Basic PSO	Advanced PSO
Results Interval(s)	0-4109	0-4109	0-4109
Cycle	UDDS	UDDS	UDDS
Cycle distance (mile)	22.33	22.39	22.34
Fuel mass (kg)	0.43	0.33	0.08
CO_2 emissions (g/mile)	60.94	45.85	10.95
Battery SOC (%)	98~60.2	98~49.38	98~28.76
Equivalent MPG	108.39	121.68	180.2
Powertrain Bidirectional path efficiency (%)	49.37	54.67	68.93
Engine ON percentage (%)	19.72%	22.85%	3.82%
Number of times Engine started	78	279	26

Table 4.10 shows the comparison of numerical results obtained from simulation by simulating the same vehicle model for identical conditions with different EMS strategies. The table shows that less gasoline was consumed for the advanced PSO strategy since it was optimized and was consuming battery as a fuel. The table also

shows that CO_2 emission into the environment was also significantly reduced over the basic PSO strategy and the PSAT strategy.

The table shows that bidirectional powertrain efficiency was improved for the advanced PSO EMS as compared to the PSAT strategy and the basic PSO EMS. It also shows the equivalent MPG comparison among the different strategies. For the advanced PSO strategy the equivalent was improved to 180.2 MPG as compared to 121.68 for basic PSO and 108.39 for the PSAT strategies. Furthermore the engine was also turned ON for lesser duration for the advanced PSO EMS as compared to other strategies. It also shows significant reduction in the number of engine starting times for advanced PSO strategy. This was one of the main objectives for the EMS which makes this EMS system implementable on real vehicles.

5. POSSIBLE REAL TIME IMPLEMENTATION OF PSO EMS

Neural networks (NN) are artificial mathematical representations of biological neural networks. They roughly imitate the human neural network system to acquire knowledge and make intelligent decisions. The main advantage of neural networks is that they can approximate the function from observations and can then be used to predict it. Hence they have been widely used for complex data or tasks that cannot be implemented easily. They are used for a variety of applications like function approximation or regression analysis, classification, including pattern recognition and data processing. They are also used in system identification and control problems in various fields.

Artificial neural networks are composed of interconnected artificial neurons which are mathematical models for information processing and providing results.

$$n = f(\sum_{i=1}^{R} w_i p_i + b) \tag{5.1}$$

where n is the output of one neuron, f is the function such as sigmoid, linear, etc., w_i are the weights corresponding to inputs p_i, R is the number of inputs and b is the constant bias.

When such neurons are stacked together and provided with the same set of inputs, they form a layer of neurons. Connecting the stack of layers of neurons, results in a network of neurons called the Multilayer Neural Network. Neural networks have an input layer and an output layer. In between these layers may be hidden layers of neurons. Figure 5.1 below shows a four layer neural network with j number of inputs and k

number of outputs. In the figure X_1, X_2, X_3,…,X_j are the inputs to the neural network whereas y_1, y_2, y_3, ….y_k are the outputs of the neural network.

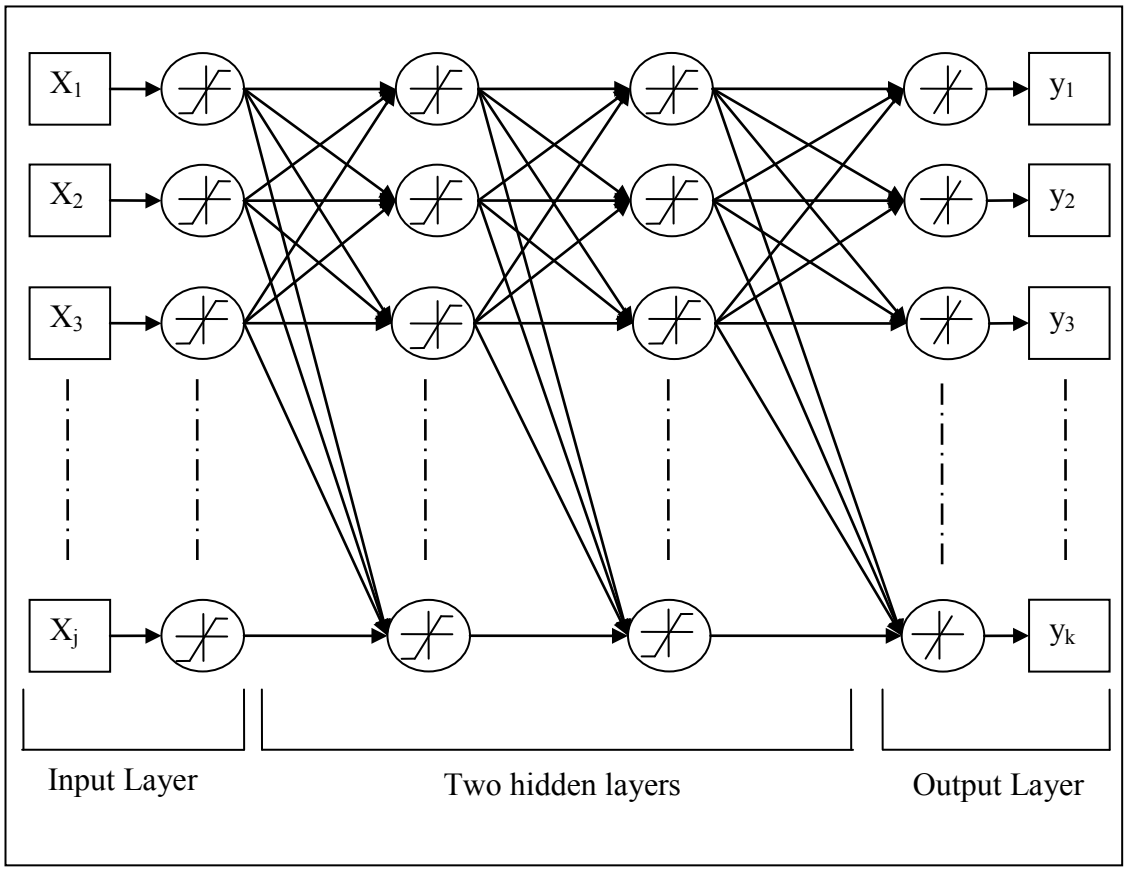

Figure 5.1 Neural Network Structure

The number of layers and neurons in each layer are determined such that the neural network becomes sufficiently non-linear according to the desired application. Initially, supervised NNs have to be trained for a known set of inputs and outputs to evaluate the weights that correspond to its inputs. Unsupervised neural networks, which train using only input patterns, also exist, but this project uses a supervised network. Often these weights are calculated using a Backpropogation Algorithm. In the Backpropogation Algorithm, the weights of each neuron are recalculated such that the errors between the outputs and desired outputs are minimized.

5.1 Simulation Setup

Implementing this neural network requires the same simulation setup of the vehicle that was used in Section 4.3.1 is used here. But the neural network was implemented in the vehicle controller of the simulation.

The goal here is to implement the optimum control strategy in real time mentioned as mentioned in Section 4.3. Due to the system complexity the control system cannot be approximated by using a single neural network, hence a dual neural network was designed. Here two identical neural networks are used. Each of these NNs is trained separately for either charge depletion or charge sustaining mode. One of the outputs from these NNs was selected based on SOC as shown in Figure 5.2. Two NNs are selected with 50 neurons in each layer for every NN. Inputs to the system are linear speed demand (v), wheel torque demand (τ), and SOC while engine speed and torque are outputs from the system. Finally these desired engine speeds and torques are used to calculate the motor and generator operating points using Equations 2.20 to 2.23. Since we had the optimal results from Section 4.3.2 for both charge depletion and charge sustaining mode we used them to train the neural networks. Here the Levenberg – Marquardt algorithm was used to train both NNs and mean squared error is used as the performance criterion for each NN. Finally, NNs are validated for their outputs which showed that they are approximately near the desired outputs.

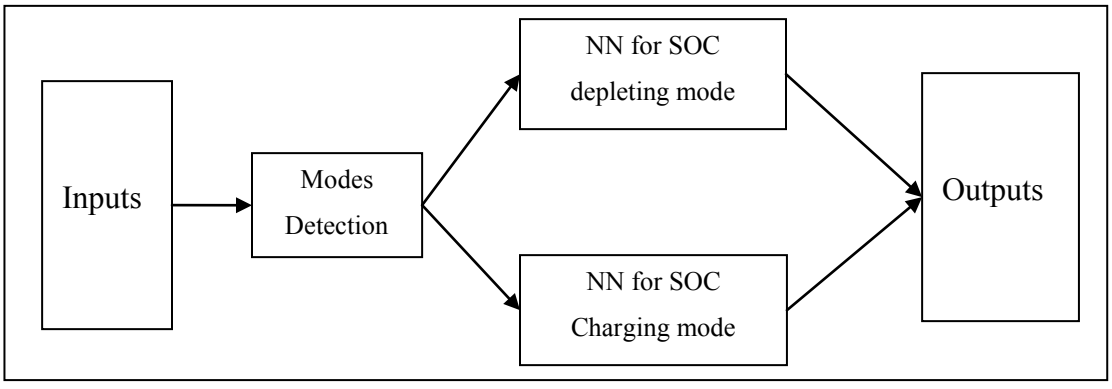

Figure 5.2 Neural Network Controller Diagram

The pair of neural networks are trained repeatedly such that the performance error i.e. mean squared error, is reduced to acceptable values by the end. Finally, the results of the neural network approach are compared with optimal results of the advanced PSO.

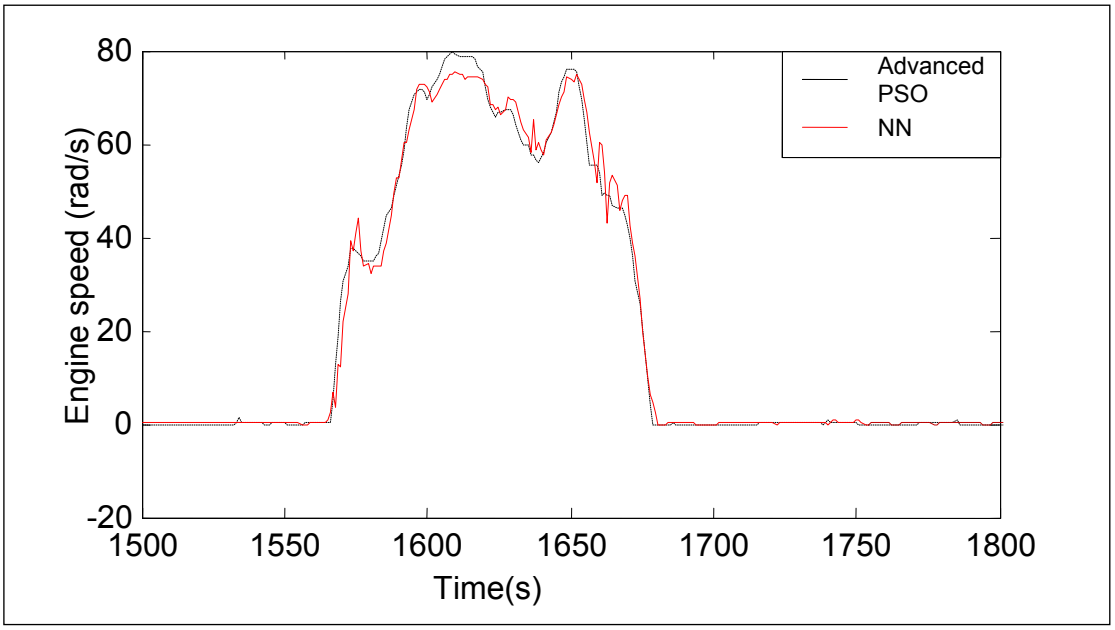

Figure 5.3 Engine Speed Comparison between Optimal Advanced PSO Results and NN Results

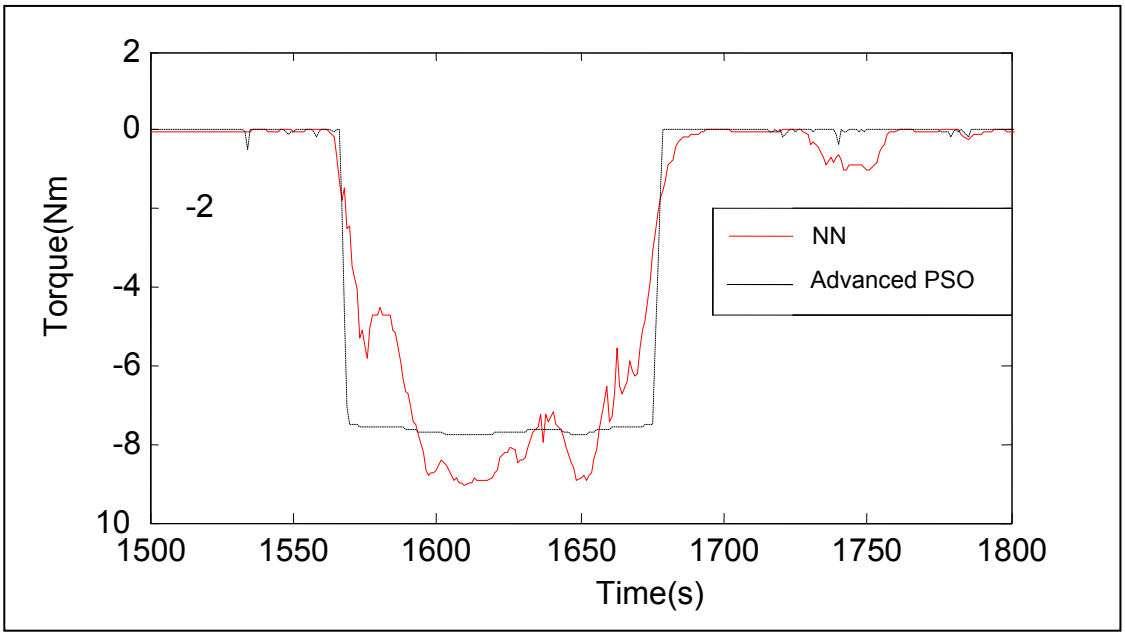

Figure 5.4 Engine Torque Comparison between Optimal Advanced PSO Results and NN Results

Figures 5.3 and 5.4 show the comparison of results of the proposed neural network and advanced PSO EMS strategy results. The two targets of engine speed and engine torques are compared to the outputs of advanced PSO results.

Finally, this neural network controller is used to simulate vehicle model using PSAT. The vehicle model is simulated for three drive cycles of UDDS.

5.2 Simulation Results and Analysis

It can be seen in Figure 5.5 the engine speed from the neural network is almost same as optimum engine speed obtained from the advanced PSO, except the part of the third drive cycle from 3000 to 4000 seconds. Because after 3000 seconds SOC is depleted to 30%, hence the vehicle entered into the SOC sustaining mode. Hence another neural network is applied. Furthermore, Figure 5.6 shows that the engine torque for the NN is almost same as the engine torque for advanced PSO EMS. But still there

are some torque and speed differences between the NN and the advanced PSO results towards the end of three drive cycles. However their impact is less on fuel economy. Therefore, it proves that this well trained NN could be used to predict the future sub-optimum engine speed and the engine torques in real time.

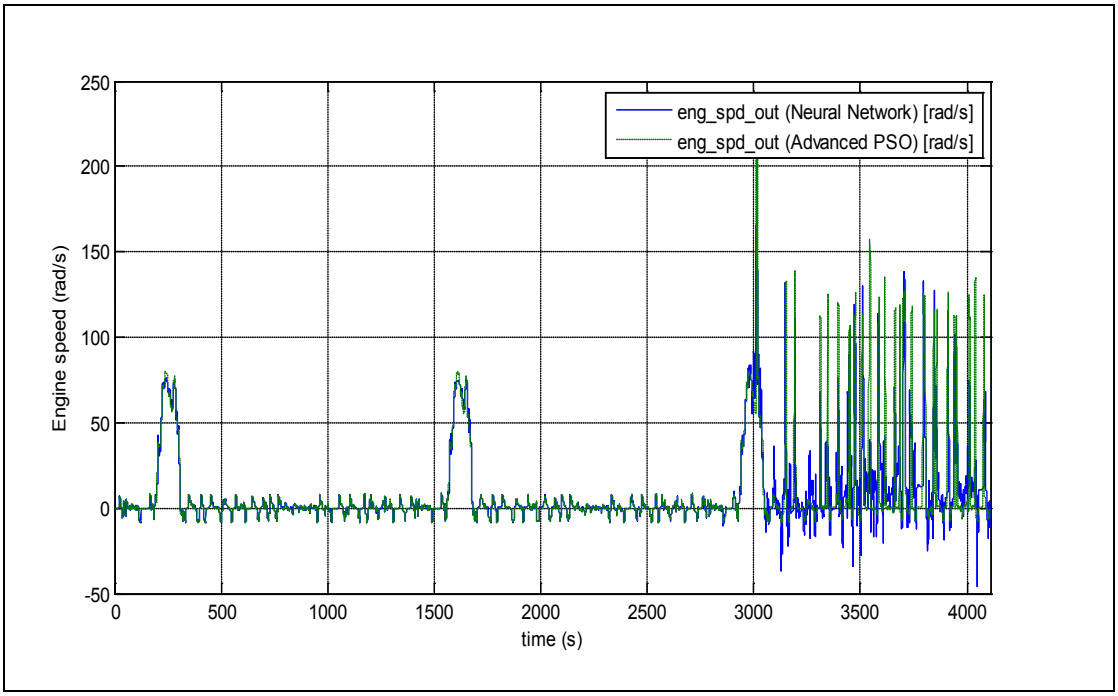

Figure 5.5 Engine Speed Comparison between Advanced PSO and NN

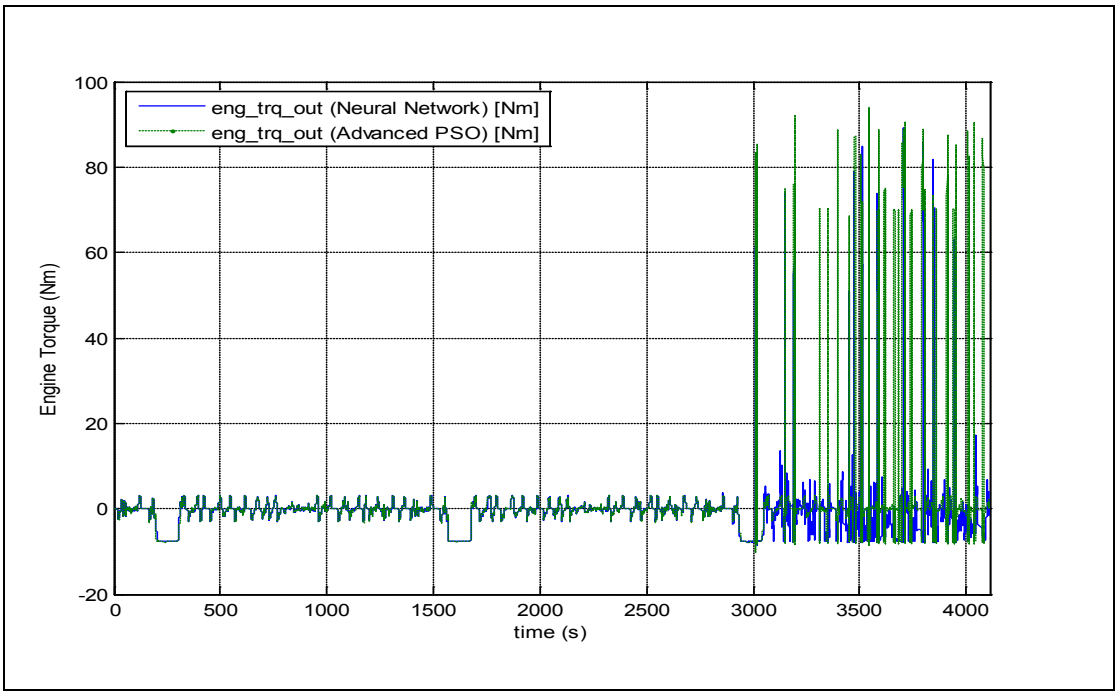

Figure 5.6 Engine Torque Comparison Between Advanced PSO and NN

Figures 5.5 and 5.6 show the engine operating points for the proposed NN and advanced PSO methods. Although there are tiny differences between these two methods, it is still tolerable to get real-time controller using the NN. Therefore, as compared to the PSO off-line method, it gives a good chance to make applicable a controller usable in commercial cars.

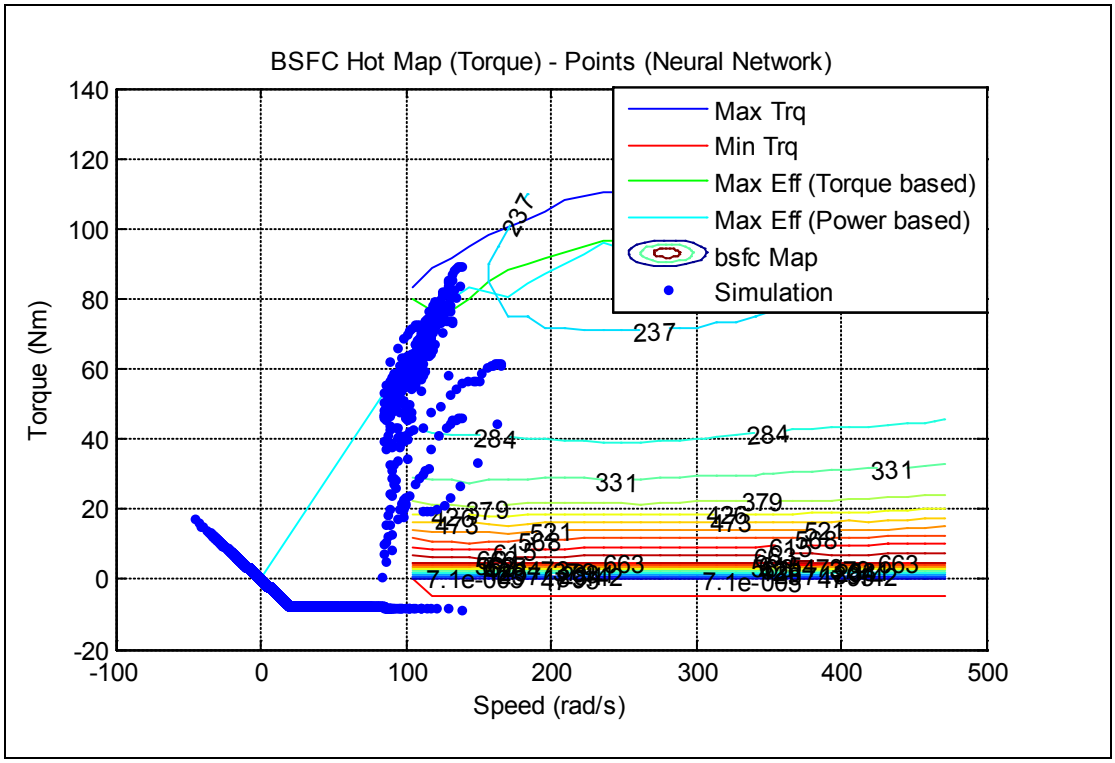

Figure 5.7 Engine Map with Neural Network

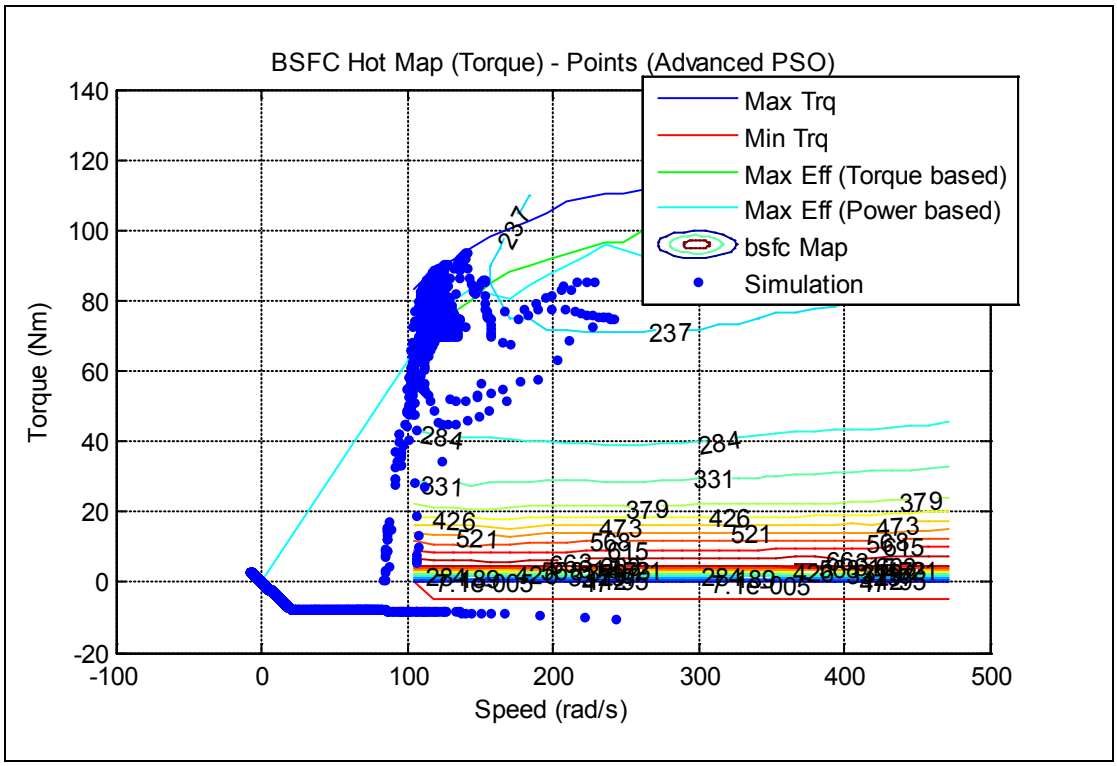

Figure 5.8 Engine Map with Advanced PSO

Figures 5.7 and 5.8 show the engine map for both the Neural Network results and the advanced PSO results. These engine operating points show that the neural network results are similar but certain operating points are different from the advanced PSO results because of the approximation.

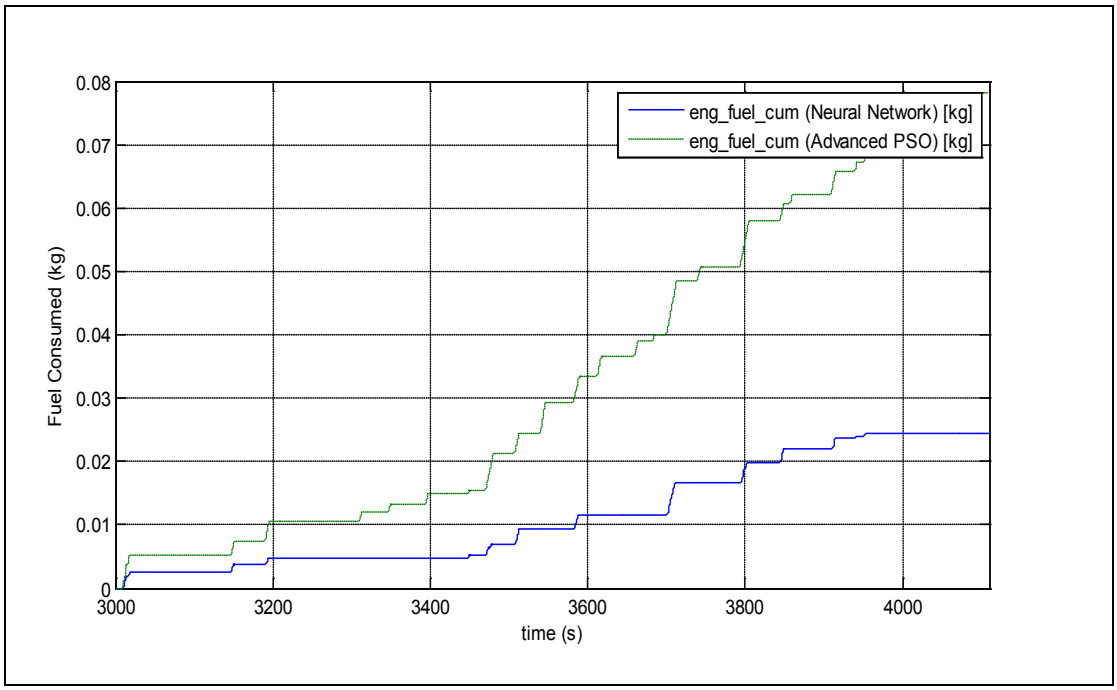

Figure 5.9 Fuel Consumption of Advanced PSO and Neural Network

Figure 5.9 shows the fuel consumption comparison between the advanced PSO and the neural network. Since the vehicle is operated under pure electric mode before 3000 seconds, fuel mass increases thereafter for both strategies. But the fuel consumption for the neural network strategy is still low because the SOC for this neural network is used to power the vehicle during this time as compared to the advanced PSO SOC. Furthermore after calculating the equivalent fuel consumption of vehicle for both the strategies it is found that the equivalent fuel economy for the vehicle with advanced PSO is 180.2 MPG whereas for the Neural network it is 180 MPG for two UDDS drive cycles. These results show that the NN provides a sub-optimal result which is expected because of the approximation of the Advanced PSO EMS.

6. CONCLUSIONS AND RECOMMENDATIONS

6.1 Conclusions

In Chapter 4 Section 4.1 a Rule Based EMS was implemented on two different vehicle models, a Powersplit drivetrain and a Parallel drivetrain model. The results of this Rule Based EMS were then compared to the Prius control strategy and Parallel control strategy in ADVISOR for different distances travelled for the UDDS drive cycle.

It was observed that with the proposed Rule Based EMS the gas mileage of the PHEV is increased by 16% over the Prius control strategy. The gas MPG of the Rule Based control Strategy was also better than that for the Parallel control strategy in ADVISOR by about 6%. The engine efficiency with Rule based EMS also increased significantly over that of Prius and Parallel control strategies. It was therefore concluded that of the Rule Based EMS was more effective for the on PHEV compared to HEV Energy Management systems on the PHEV for the same battery capacity.

In Section 4.2 the gradient free algorithm Particle Swarm Optimization was used to improve the fuel economy of the vehicle. So a simplified model of the power split drivetrain of an HEV was developed. This model was used along with PSO to obtain the near optimal operating points of the engine while satisfying various component physical constraints, as well as vehicle performance constraints. The resulting optimum operating points of the engine obtained from PSO were then given as input to the PSAT model. The results from the PSAT model were compared with the PSAT, a default strategy for identical power split HEV drivetrain.

The results showed significant improvement in MPG for the vehicle with the PSO strategy compared to an identical vehicle configuration for the PSAT strategy for almost the same electrical consumption. The improvements showed enhancement in fuel economy which was the main objective of the study. Meanwhile, there was also an increase in the powertrain bidirectional path efficiency of the vehicle. During the simulation it was also observed that performance of the vehicle was improved slightly while comparing with the PSAT strategy counterpart.

The operating points obtained in this section were only for blended mode strategy. Here both engine and/or battery can be used to drive the vehicle even if the battery has sufficient potential to drive it which was not desirable for short distances. Hence control strategy was defined accordingly for shorter distances. For the PHEV vehicle, the blended strategy described above was not very effective since it had a large battery. This stored electrical energy, and should be have been used for short drives to get better MPG. In Section 4.3 the new optimized strategy based on this concept was obtained.

In Section 4.3 the advanced PSO problem which was formulated in Section 3.3.1 was implemented using a simplified model developed from the modeling equations of each component from Chapter 2. These results were used in the PSAT model for the powersplit drivetrain to provide better accuracy and analysis.

The simulation results showed that optimum results of advanced PSO strategy provided good results over the PSAT strategy and the basic PSO strategy. These optimum results were first obtained offline and then implemented on the model. Since the optimization process took a long time to evaluate optimum points, it could not be implemented in real time. To overcome this problem a neural network solution to implement this real time control strategy was shown in Chapter 5.

In Chapter 5, the optimal results obtained from the advanced PSO strategy were used to train the neural network.

The results from the neural network were approximately the same for the entire PSO results, thus near optimal control was obtained.

So a possible real-time implementable strategy has been designed step wise from the rule based EMS to a real-time sub-optimal strategy.

6.2 Recommendations for Future

In the future, more work can be done to improve the Optimized Energy Management System as shown below.

- When comparing the neural network results with the advanced PSO results, it can be seen that in charge sustaining mode there are some errors in the neural network output as compared to the advanced PSO output. These errors can be reduced by training the neural network with better training sets.
- In [19] it is mentioned that the local version of PSO can often provides better results as compared to the global version. The near optimal results obtained from the advanced PSO are obtained using the global version of PSO. By using the local version of PSO the near optimal results obtained for advanced PSO may be improved.
- The Energy Management System is designed based on prior knowledge of the drive cycle. In future this EMS can be improved by a neural network or fuzzy logic such that it can provide real time results independent of prior knowledge of the drive cycle.

LIST OF REFERENCES

LIST OF REFERENCES

[1] D. Karbowski, A. Rousseau, S. Pagerit and P. Sharer, "Plug-in vehicle control strategy: from global optimization to Real-time Application," Electric Vehicle Symposium EVS23, Anaheim, California, Dec. 2-5. 2007.

[2] A. Rousseau, S. Pagerit and D. Gao, "Plug-in hybrid electric vehicle control strategy parameter optimization," EVS23, Anaheim, California, Dec. 2-5. 2007.

[3] Q. Cao, S. Pagerit, R. B. Carlson and A. Rousseau, "PHEV hymotion Prius model validation and control improvements," EVS23, Anaheim, California, Dec. 2-5. 2007.

[4] X. Wu, B. Cao, J. Wen and Y. Bian, "Particle swarm optimization for plug-in hybrid electric vehicle control straegy parameter," IEEE Vehicle Power and Propulsion Conference (VPPC), Harbin, China, Sept. 3-5. 2008.

[5] Q. Gong, Y. Li and Z. Penng, "Optimal power management of plug-in HEV with intelligent transportation system," Advanced Intelligent Mechatronics 2007 IEE/ASME international conference, Zurich, Switzerland, 4-7 Sept. 2007, pp 1-6.

[6] B. Baumann, G. Washington, B. Glenn and G. Rizzoni, "Mechatronic design and control of hybrid electric vehicle," IEEE/ASME Transactions on Mechtronics, Vol. 5, No. 1, Mar. 2000, pp. 58-72.

[7] Y. Gao and M. Ehsani, "Design and control methodology of plug-in hybrid electric vehicles," IEEE Vehicle Power and Propulsion Conference (VPPC), Harbin, China, September 3-5. 2008.

[8] L. Sun, R. Liang and Q. Wang, "The control strategy and system preference of plug-in HEV," IEEE Vehicle Power and Propulsion Conference (VPPPC), Harbing, China, September 3-5. 2008.

[9] S. Moura, D. Callaway, H. Fath and J. Stein, "Impact of battery sizing on stochastic optimal power management in plug-in hybrid electric vehicles,"IEEE Int. Conf. Vehicular Electronics and Safety, Columbus, Ohio, USA, 22-24 Sept. 2008

[10] H. Borhan, A. Vahidi, A. Phillips, M. Kuang and I. Kolmanovsky, "Predictive energy management of a power-split hybrid electric vehicle," American Control Conference, St. Louis, MO, June 10-12. 2009.

[11] Y. Bin, Y. Li, Q. Gong and Z. Peng, "Multi-information integrated trip specific optimal power management for plug-In hybrid electric vehicles," American Control Conference, St. Louis, MO, June 10-12. 2009.

[12] Q. Gong, Y. Li, Z and Peng, "Power management of plug-in hybrid electric vehicles using neural network based trip modeling," American Control Conference, St. Louis, MO, June 10-12. 2009.

[13] M. Mohebbi and M. Farrokhi, "Adaptive neuro control of parallel hybrid electric vehicles," Int. J. Electric and Hybrid Vehicles, Vol. 1, No.1. 2007, pp. 3-19.

[14] B. Baumann, G. Rizzoni and G. Washington, "Intelligent control of hybrid vehicles using neural networks and fuzzy logic," Electronic Engine Controls, Vol. SP-1356, 1998, pp.125-133.

[15] J. Moreno, J. Dixon and M. Ortuzar, "Energy management system for an hybrid electric vehicle, using ultracapacitors and neural networks," Industrial Electronics, IEEE Transactions, Vol. 53, Issue-2, Apr. 2006, pp. 614-623.

[16] PSAT v6.2, Documentation, Argonne National Laboratory (ANL).

[17] ADVISOR v3.1 Documentation, National Renewable Energy Laboratory, (NREL).

[18] J. Kennedy and R. Eberhart, "Particle swarm optimization," Neural Networks, Proceedings, IEEE International Conference, Piscataway, NJ, Vol., 5, 1995, pp. 1942-1948.

[19] R. Eberhart and J. Kennedy, "A new optimizer using particle swarm theory," Proceedings of the sixth international symposium on micro machine and human science, IEEE Service Center, Piscataway, NJ, Nagoya, Japan, 1995, pp. 39-43.

[20] X. Hu and R. Eberhart, "Solving constrained nonlinear optimization problems with particle swarm optimization," Proceedings of the Sixth World Multi Conference on Systemics, Cybernatics and Informatics, Orlando, Florida, 2002.

[21] G. Toscano, Pulido and C. Coello, "A constraint handling mechanism for particle swarm optimization," Evolutionary Computation, Vol. 2, 2004, pp. 1396-1403.

[22] K. Parsopuulos and M. Vrahatis, “Particle swarm optimization method for constrained optimization problems,” Intelligent Technologies- Theory and application, IOS Press, 2002, pp. 214-220.

[23] J. Kennedy, R. Eberhart and Y. Shi, “Swarm intelligence,” Morgan Kaufmann, 2001, San Francisco, CA.

[24] http://www.swarmintelligence.org/. Last accessed on 28 November 2009.

APPENDIX

APPENDIX COMPARED STRATEGIES

A.1 Rule Based EMS for Prius control strategy in ADVISOR

The Prius is a combination of both parallel and series powertrains. For this powertrain, the continuous variable transmission (CVT) is used which consists of a planetary gear set connected to the motor, generator and engine. The planetary gear set provides speed coupling between the engine and the generator. Also there exists a torque coupling between the engine and motor.

In the Rule Based Energy Management Control strategy which is being used by the Advisor model for the Prius, the power generated by the ADVISOR model for the Prius, the power generated by the engine is controlled power while the remaining power is provided by the motor. The engine ON/OFF condition is dependent on the state of charge (SOC) of the battery, the power requested, the vehicle speed and the engine coolant temperature.

The various engine operating modes are selected based on the following set of rules.

a) If the SOC of battery is enough the power requested can be provided by the battery, the vehicle is operating at low speed and the coolant temperature is acceptable, then the vehicle is operated only in electric mode.
b) If the engine is ON and the state of charge of the battery is above the targeted state of charge then the engine and the motor both provide the requested power demand.
c) If the state of charge of the battery goes below the targeted state of charge then the engine provides extra power to charge the battery and also powers the vehicle.

d) If the power requested by the vehicle is negative and the engine is OFF then the entire negative requested power is stored in the battery using regenerative braking.

A.2 Rule Based EMS for Parallel control strategy in ADVISOR

In rule based strategy EMS control strategy for the parallel drivetrain the engine power is controlled and the remaining power is delivered by the motor. But in the Parallel powertrain the Gearbox is used. Here the following control strategy is used.

a) If the vehicle speed is below the electric launch speed limit and the state of charge of battery is greater than the lower limit then it will be powered entirely by the motor in EV mode.
b) If the power required by the vehicle exceeds the maximum power that can be provided by the engine and the State of Charge of the battery is more than its power limit then the remaining power is provided by the motor.
c) When the power required by the vehicle is negative all the negative power is stored by the battery via regenerative braking.
d) The engine may also turn off if the torque required drops below a certain limit, i.e. off torque limit in the Figure A.1, if the state of charge is greater than the lower limit of state of charge.

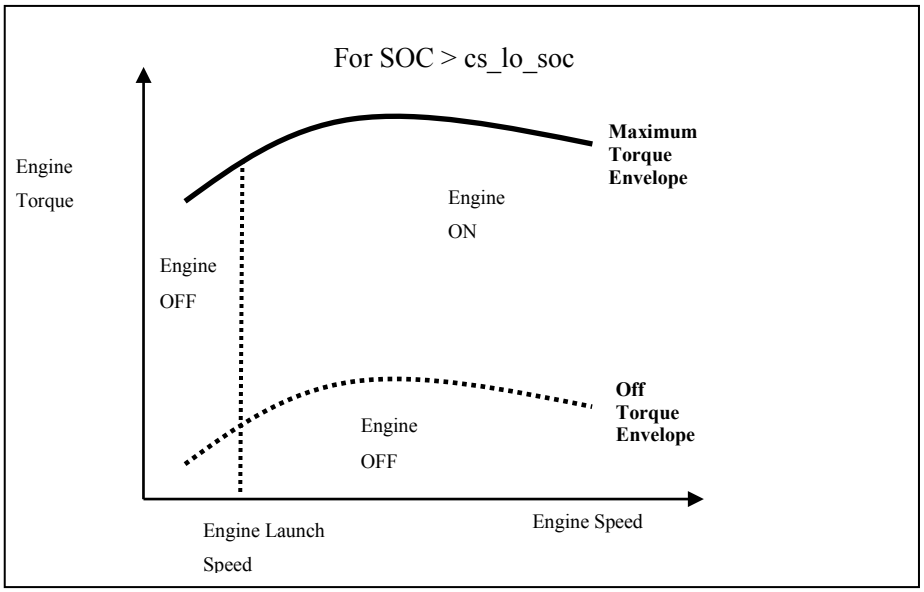

Figure A.1 Charge Depletion Strategy for Parallel Strategy [17]

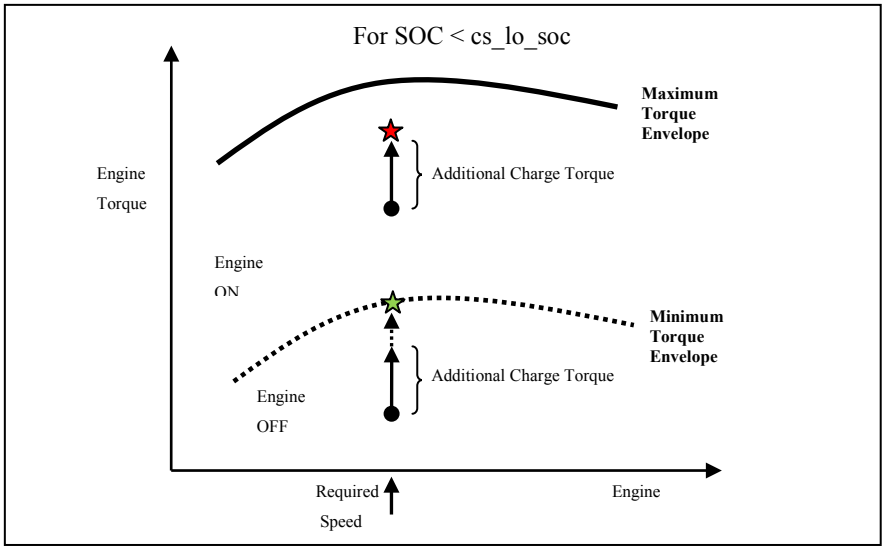

Figure A.2 Charge Sustaining Strategy for Parallel Strategy [17]

If the state of charge of the battery drops below its lower limit then the engine provides the extra power which is then used to charge the battery as shown in Figure A.2 while operating above the minimum torque envelope.